uOttawa

L'Université canadienne
Canada's university

FACULTÉ DES ÉTUDES SUPÉRIEURES ET POSTOCTORALES

uOttawa

L'Université canadienne
Canada's university

FACULTY OF GRADUATE AND POSDOCTORAL STUDIES

Melanie McKay
AUTEUR DE LA THÈSE / AUTHOR OF THESIS

M.Sc. (Mathematics)
GRADE / DEGREE

Department of Mathematics and Statistics
FACULTÉ, ÉCOLE, DÉPARTEMENT / FACULTY, SCHOOL, DEPARTMENT

Iterative Methods for Incompressible Flow

TITRE DE LA THÈSE / TITLE OF THESIS

Dr. R. Vaillancourt
DIRECTEUR (DIRECTRICE) DE LA THÈSE / THESIS SUPERVISOR

Dr. Y. Bourgault
CO-DIRECTEUR (CO-DIRECTRICE) DE LA THÈSE / THESIS CO-SUPERVISOR

EXAMINATEURS (EXAMINATRICES) DE LA THÈSE / THESIS EXAMINERS

Dr. B. Dionne

Dr. D. Amundsen

Gary W. Slater
Le Doyen de la Faculté des études supérieures et postdoctorales / Dean of the Faculty of Graduate and Postdoctoral Studies

Iterative Methods for Incompressible Flow

Melanie McKay

Thesis submitted to the Faculty of Graduate and Postdoctoral Studies
in partial fulfillment of the requirements for the degree of Master's of Science in
Mathematics [1]

Department of Mathematics and Statistics
Faculty of Science
University of Ottawa

[1]The M.Sc. program is a joint program with Carleton University, administered by the Ottawa-Carleton Institute of Mathematics and Statistics

Your file Votre référence
ISBN: 978-0-494-51650-8
Our file Notre référence
ISBN: 978-0-494-51650-8

Abstract

The goal of this thesis is to illustrate the effectiveness of iterative methods on the discretized Navier–Stokes equations. The standard lid-driven cavity in both 2-D and 3-D test cases are examined and compared with published results of the same type. The numerical results are obtained by reducing the partial differential equations (PDEs) to a system of algebraic equations with a stabilized P1-P1 Finite Element Method (FEM) in space. Gear's Backward Difference Formula (BDF2) and an adaptive time stepping scheme utilizing a first order Backward Euler (BE) startup and BDF2 are then utilized to discretize the time derivative of the Navier–Stokes equations. The iterative method used is the Generalized Minimal Residual (GMRES) along with the selected preconditioners Incomplete LU Facorization (ILU), Jacobi preconditioner and the Block Jacobi preconditioner.

Contents

List of Figures

List of Tables

Chapter 1

Elementary Concepts

Numerical methods have a vast range of applications which include approximating partial differential equations that appear in the study of fluid mechanics. The governing equations of motion in the study of fluids are the Navier–Stokes equations, a system of partial differential equations due to Claude-Louis Navier and George Gabriel Stokes. The problem of efficiently and accurately solving the Navier–Stokes equations is not a simple process and is an on-going task that is being refined year after year. The goal of this thesis is to analyze some of these methods in some simple 2D and 3D test cases. Simulating flows has many applications such as blood flow in the circulatory system and air flow in the respiratory system just to name a few. A relevant example would be to analyze the effects of installing a ventricular assist device, which acts as a mechanical pump for hearts that are too weak to pump the blood.

A first glance at the Navier–Stokes equations in their continuous form readily shows difficulties, especially when the domain, boundary conditions and initial conditions become complex. As we shall soon see, many methods have been derived to tackle this problem with promising results. Discretization of the equations via a Finite Element Method (FEM) aids in reducing them to a system of algebraic differential equations

and then an appropriate time stepping scheme can be chosen to further reduce our problem to a system of nonlinear iterative equations. One can then linearize the equations via a method such as Newton's method. Once the equations have been linearized methods like the generalized minimal residual method (GMRES), least squares method or in the case of a symmetric Jacobian matrix, the conjugate gradient method (CG) or conjugate residual method (CR) may be used. In our case the Navier–Stokes equations generate a non-symmetric Jacobian matrix which leaves us with few choices for an iterative solver. GMRES is a common choice here. Even once linearized, other tricks are required. One being the use of a preconditioner. Preconditioners are used when the condition number of the linear system of equations is too large. Generally, a preconditioner will not require many extra computations but will speed up the convergence.

In this first chapter we will introduce the Navier-Stokes Equations in their continuous form and outline the process of using a finite element method to reduce the equations to a fully discretized system of nonlinear algebraic equations.

1.1 Navier–Stokes Equations

Given a flow problem in $\mathbb{R}^d$ we shall set $u = (u_1, \ldots, u_d)^T$ to be the velocity vector of the flow and p the pressure field. Let $\Omega \subset \mathbb{R}^d$ be a bounded domain with boundary Γ, then the Navier–Stokes equations for incompressible flow in their non-dimensional form are

$$\begin{aligned} &\frac{\partial u}{\partial t} + u \cdot \nabla u + \nabla p - \mathrm{Re}^{-1}\Delta u = f && \text{in } \Omega, \\ &\nabla \cdot u = 0 && \text{in } \Omega, \\ &u = u_\Gamma && \text{on } \Gamma, \\ &u(\cdot, 0) = u_0 && \text{in } \Omega. \end{aligned} \tag{1.1.1}$$

The first equation is called the momentum equation, the second is the conservation of mass and the third and fourth are the boundary and initial conditions, respectively. The non-dimensional parameter Re represents the Reynolds number and is defined as $\mathrm{Re} = VL/\nu$ where V and L are the characteristic velocity and length of the flow, respectively. The parameter ν is the kinematic viscosity, the function f is given and represents a body force such as gravity, u_Γ is the prescribed velocity on the boundary Γ of the domain Ω and u_0 is the initial velocity.

Now we want to state the Navier–Stokes equations in variational form. Let $L^2(\Omega)$ be a second order Lebesgue space on Ω. We define the Sobolev space $H_0^1(\Omega) = \{u \in L^2(\Omega) : \partial u \in L^2(\Omega), u = 0 \text{ on } \Gamma\}$ and the Lebesgue space $L_0^2(\Omega) = \{q \in L^2 : \int_\Omega q = 0\}$. We shall require test functions $v \in [H_0^1(\Omega)]^d$ and $q \in L_0^2(\Omega)$. We then multiply the conservation of momentum and mass equations by v and q, respectively, and integrate by parts over Ω yielding a variational form of the problem (1.1.1): Find $u \in \{w \in [H^1(\Omega)]^d : w|_\Gamma = u|_\Gamma\}$ and $p \in L^2_{\int=0}(\Omega)$ such that

$$\begin{aligned} &\frac{d}{dt}(u, v) + c(u, u, v) + b(v, p) + a(u, v) = (f, v) && \text{for any } v \in [H_0^1(\Omega)]^d, \\ &b(u, q) = 0 && \text{for any } q \in L_0^2(\Omega). \end{aligned} \tag{1.1.2}$$

The above products are outlined in [7] and defined to be

$$\begin{aligned} (u, v) &= \int_\Omega u \cdot v \, dx, & c(u, v, w) &= \textstyle\int_\Omega (u \cdot \nabla v) \cdot w \, dx, \\ b(q, v) &= -\int_\Omega q \nabla \cdot v \, dx, & a(u, v) &= \tfrac{1}{\mathrm{Re}} \textstyle\int_\Omega \nabla u : \nabla v \, dx, \end{aligned} \tag{1.1.3}$$

where $\nabla u : \nabla v = \sum_{i,j} \frac{\partial u_i}{\partial x_j} \frac{\partial v_i}{\partial x_j}$.

The Navier–Stokes equations in their continuous form are of limited use until they are fully discretized. For this, we use a Galerkin type finite element method (GFEM) that will be discussed in the next section. The variational form of the Navier–Stokes equations is our first bridge to this numerical approximation.

1.2 Discretization with Finite Element Method

To solve equations (1.1.1) we must use a finite element method for the velocity and the pressure terms. In order to stabilize these elements a Streamline-Upwind Petrov Galerkin / Pressure–Stabilized Petrov Galerkin (SUPG/PSPG) formulation is used. A paper by P. Kjellgren [11] explains the need for the SUPG formulation saying that the convective terms of the Navier–Stokes equations are the cause for some numerical problems involving the appearance of oscillatory solutions and a means for stabilizing these is with upwinding. Upwinding is a scheme that aids in properly simulating the direction of propagation of a fluid flow. PSPG is required to bypass Brezzi–Babuska conditions [4],[7]. In the following section we shall first see what is a mesh and how to obtain the SUPG/PSPG formulation of (1.1.1). Following this we will obtain the fully discretized Navier–Stokes equations using Galerkin's method. For this let us first define what is a *mesh.*

Definition 1.2.1 *[4, p. 32][Mesh] Let Ω be a domain in $\mathbb{R}^d$. A mesh is a union of a finite number N of compact, connected, Lipschitz sets K_m with non-empty interior $\mathring{K}_m$ such that $\{K_m\}_{1 \le m \le N}$ forms a partition of Ω, i.e.,*

$$\overline{\Omega} = \bigcup_{m=1}^{N} K_m \qquad \text{and} \qquad \mathring{K}_m \cap \mathring{K}_n = \emptyset \text{ for } m \neq n.$$

Denote the mesh by $\mathcal{T}_h$ where $h = \max_{1 \le i \le N} \text{diam} K_i$

In practice, a mesh is generated from a reference finite element and a set of geometric transformations mapping the reference cell $\widehat{K}$ to the rest of the mesh cells. Let $K \in \mathcal{T}_h$ be any cell in the mesh then the geometric transformation is typically denoted by $T_k : \widehat{K} \to K$. For our problem of discretizing the Navier–Stokes equations we shall use a mesh consisting of triangles or tetrahedra, making a triangulation of the domain.

The SUPG/PSPG formulation is a Petrov–Galerkin formulation in which a weight function is applied to all the terms in the Navier–Stokes equations. Let $\mathcal{T}_h$ be a triangulation of the domain Ω into elements K with diameter h_k. We next define the spaces of test functions for pressure and velocity as

$$
\begin{aligned}
Q_h &= \{q_h | q_h \in P_h^1\}, \\
V_h &= \{u_h | u_h \in [P_h^1]^d, u_h = \Pi_h u_\Gamma \text{ on } \Gamma_h\}, \\
V_{h0} &= \{v_h | v_h \in [P_h^1]^d, v_h = 0 \text{ on } \Gamma_h\},
\end{aligned}
$$

where P_h^1 is the set of continuous P^1 finite elements on the mesh $\mathcal{T}_h$ and Π_h the usual P^1 Lagrange interpolation operator. The SUPG/PSPG formulation of the semi-discretized problem (1.1.1) is as follows: Find $(u_h, p_h) \in V_h \times Q_h$ such that for all $(v_h, q_h) \in V_{h0} \times Q_h$

$$
\begin{aligned}
&\tfrac{d}{dt}(u_h, v_h) + b(u_h, u_h, v_h) + a(u_h, v_h) - (\nabla \cdot v_h, p_h) + (q_h, \nabla \cdot u_h) + ST = (v_h, f), \\
&u_h(\cdot, 0) = \Pi_h u_0(\cdot) \text{ in } \Omega.
\end{aligned}
\tag{1.2.1}
$$

The PSPG/SUPG stabilization term is given by

$$
ST = \sum_{K_h \in \mathcal{T}_h} \int_{K_h} (\tau_{\text{SUPG}} u_h \cdot \nabla v_h + \tau_{\text{PSPG}} \nabla q_h) \cdot R(u_h, p_h)\, dx,
$$

where $R(u_h, p_h) = \frac{\partial}{\partial t}u_h + u_h \cdot \nabla u_h - \nu \Delta u_h + \nabla p_h - f$ is the residual of the momentum equation. The coefficients τ_{SUPG} and τ_{PSPG} are defined as

$$\tau_{\text{SUPG}} := \alpha_u \frac{h_k}{2\|u_h\|}\xi, \qquad \tau_{\text{PSPG}} := \alpha_p \frac{h_k}{2\|u_h\|}\xi,$$

where ξ is a function of the element's Reynolds number $R_K = \frac{0.5\|u_h\|h_k}{\nu}$ and is given by $\xi(R_K) = \max\{0, \min\{\frac{R_K}{3}, 1\}\}$. The typical values for α_u and α_p are between 1 and 5.

We shall next use locally linear shape functions that are determined by the value at the vertices of the triangle or tetrahedron. Essentially we are re-writing our problem in a new basis, that of our local shape functions. This will simplify the calculations needed to solve for the terms in the variational form of the Navier–Stokes equations (1.1.2). The GFEM uses P^1 local shape functions, say $\{\theta_1, \ldots, \theta_n\}$ for the velocity and $\{\psi_1, \ldots, \psi_m\}$ for the pressure terms, and estimates u by u_h with $u_h = \sum_{j=1}^{n} U_j \theta_j$, with $U_j = (U_{j1}, \ldots, U_{jd}] \in \mathbb{R}^d$ and similarly estimates p by p_h with $p_h = \sum_{j=1}^{m} P_j \psi_j$ with $P_j \in \mathbb{R}$. We shall introduce two new vectors, $U = [U_1, \ldots, U_n]^T$ and $P = [P_1, \ldots, P_j]^T$. The next step is to replace these estimates into (1.2.1). Now since the test function v_h is arbitrary in V_{h0} we can choose it to be one of our shape functions, say $\theta = \theta_i$, $i = 1, \ldots, n$ for each velocity component. Let us look at what happens to our first product $(u_h, v_h) = \int_\Omega u_h \cdot v_h \, dx$:

$$\begin{aligned}
&\int_\Omega u_h \cdot v_h \, dx = \int_\Omega \left(\sum_{j=1}^{n} U_j \theta_j \cdot \theta \right) dx \\
&= \sum_{j=1}^{n} \int_\Omega U_j \theta_j \theta_i \, dx, \quad \text{where } i = 1, \ldots, n \\
&= U_1 \int_\Omega \theta_1 \theta_i \, dx + \cdots + U_n \int_\Omega \theta_n \theta_i \, dx, \quad \text{where } i = 1, \ldots, n \\
&= M_{ij} U
\end{aligned}$$

where M_{ij} is an $n_u \times n_u$ matrix whose ij^{th} entry is $\int_\Omega \theta_i \theta_j \, dx$

We shall set $q_h = 0$ and let $\dot{U}$ represent the time derivative. Applying similar techniques as above to the other terms in equation (1.2.1) we obtain the following discretized form as in [11]:

$$\begin{aligned} M\dot{U} + N(U) + KU - B^T P &= F, \\ BU &= 0, \end{aligned} \tag{1.2.2}$$

where the matrices M, N, K, B^T and B are the mass, convection, diffusion, gradient and divergence matrices, respectively, and F is a vector representing an external force. The ij^{th} entries of the matrices corresponding to those just mentioned are defined as

$$\begin{aligned} M_{ij} &= \int_\Omega \theta_i \cdot \theta_j \, dx, \\ N_{ij} &= \int_\Omega (u_h \cdot \nabla\theta_i) \cdot \theta_j \, dx \\ K_{ij} &= \int_\Omega \nabla(\theta_i) : \nabla(\theta_j) \, dx, \\ B_{ij}^T &= \int_\Omega \psi_j div(\theta_i) \, dx. \end{aligned}$$

From the variational form we used a SUPG/PSPG finite element method to obtain equation (1.2.2); however there is still a time derivative in this equation that needs to be dealt with. This is where numerical methods in ordinary differential equations (ODE's) will be useful since our only independent variable is now that of time. There are several different time-stepping schemes that can be used; Gresho[6] and [7], provides very good resources for instance, for choosing appropriate numerical methods when dealing with PDE's and outlines some good choices for dealing with advection-diffusion problems such as the Navier–Stokes problem. The methods that were used in this research will be outlined in Chapter 2.

Chapter 2

Iterative Methods Used for Solving the Discretized Navier–Stokes Equations

Now that we have used the FEM in space, chapter two will introduce the numerical methods used to approximate the time derivative as well as the iterative methods used to solve the fully discretized Navier–Stokes equations. The following diagram shows a skeleton of the discretization process.

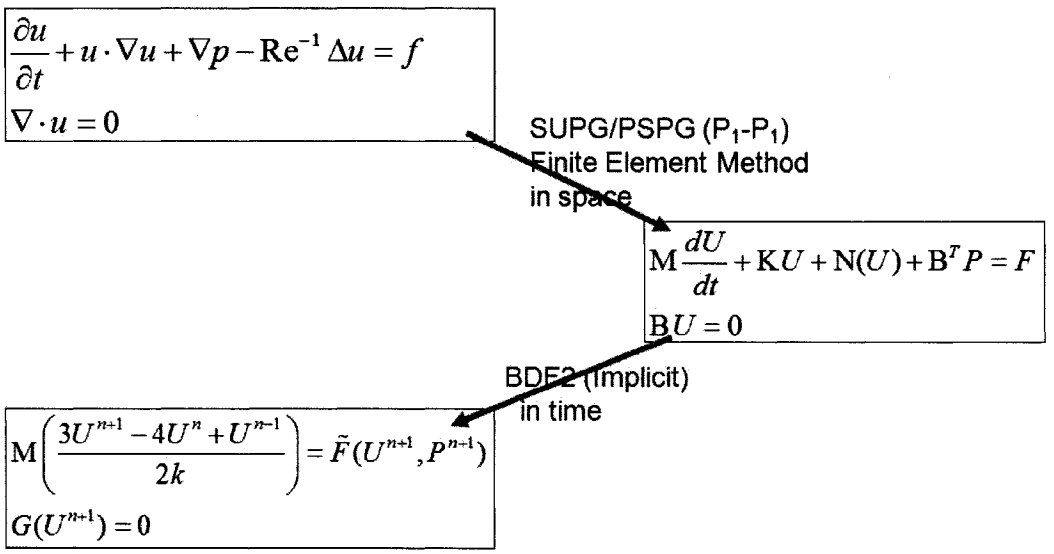

2.1 Time Stepping Schemes

Several numerical methods are available for solving ordinary differential equations. To name a few there are Backward Euler (BE), Forward Euler (FE), Adams–Bashforth (AB), Runge–Kutta methods (RK), Backward Difference Formula (BDF), etc... Hairer [8][9] as well as Gresho [6][7] present and analyze many of these time-stepping schemes. A common choice that is used when dealing with the Navier–Stokes equations is the Backward Difference Formula of order 2 (BDF2) as Gresho suggests in [7].

First let us take a look at how BDF2 works with a constant time step. We shall let $\frac{du}{dt} = \dot{u}$ and Δt be the time step size. Then,
given $\dot{u} = f$ and $u(0) = u_0$,

$$\dot{u}_{n+1} \approx \frac{3u_{n+1} - 4u_n + u_{n-1}}{2\Delta t}. \tag{2.1.1}$$

This method is, however, not self-starting due to the need of two previous terms, u_n and u_{n-1}, to find the solution at iteration $n+1$. This is why we implement it with a first order BE startup. First order BE has the following form:

$$\dot{u}_{n+1} \approx \frac{u_{n+1} - u_n}{\Delta t}. \tag{2.1.2}$$

BE is used with u_0 to get u_1 and then after this first step we have enough values to use BDF2 for all remaining steps. If we apply BDF2 to the Navier–Stokes equations we have the following implicit scheme for a difference algebraic equation (DAE):

$$\begin{aligned} &M\left(\frac{3U_{n+1} - 4U_n + U_{n-1}}{2\Delta t}\right) + KU_{n+1} + N(U_{n+1})U_{n+1} - B^T P_{n+1} = F_n, \\ &BU_{n+1} = 0, \end{aligned} \tag{2.1.3}$$

that needs to be solved at each time step.

2.2 Iterative Solvers

Iterative solvers are essential tools for solving large systems of algebraic equations like the discretized Navier–Stokes equations. Many methods have been developed like descent methods, gradient methods and Newton's method. Many of these methods are described in Saad's book [12]. Due to the nonlinearity of the discretized Navier–Stokes equations, Newton's method is a common starting point as it transforms the problem into a linear system. This is the method that will be used in this thesis.

Given the nonlinear function $G(U) = 0$ and an initial guess of the solution U_0, the general step for a Newton iteration is

$$\begin{aligned} &[DG(U_n)]\delta U = -G(U_n) \\ &U_{n+1} = U_n + \delta U. \end{aligned} \tag{2.2.1}$$

From equation (2.1.3) we shall set

$$G(U_{n+1}, P_{n+1}) = \begin{bmatrix} M\left(\frac{3U_{n+1} - 4U_n + U_{n-1}}{2\Delta t}\right) + KU_{n+1} + N(U_{n+1}) + B^T P_{n+1} - F_n \\ BU_{n+1} \end{bmatrix}.$$

Applying Newton's method to G yields

$$\begin{aligned}&\left[\left(\frac{3}{2\Delta t}M + K + DN(U_n)\right)\delta U_{n+1} - B^T\delta P_{n+1}\right] U_{n+1} = \tilde{G}(U_n),\\ &B\delta U_{n+1} = 0,\end{aligned} \tag{2.2.2}$$

where $U_{n+1} = U_n + \delta U_{n+1}$ and $P_{n+1} = P_n + \delta P_{n+1}$.

Now that the system has been linearized we must next choose an appropriate iterative solver. In PETSC there are few options for this choice as the matrix obtained in (2.2.2) is non-symmetric. The method available that best applies to the discretized Navier–Stokes equations is the Generalized Minimal Residual Method (GMRES). It is a generalization of the conjugate gradient algorithm as in [4, p. 405] and [12, p. 144–169]. In order to understand how GMRES works we need first to understand projection-based iterative methods.

Before looking at the iterative methods let us quickly observe a direct method commonly used called LU factorization. Consider the system $Ax = b$. The first step is to use Gaussian elimination to re-write the matrix A in the form

$$A = LU$$

where L and U are lower and upper triangular matrices, respectively. Now there are two steps to solve our linear system:

(i) Solve $Lx' = b$,

(ii) Solve $Ux = x'$.

For stability, pivoting needs to be used. Efficient as this method may be at getting accurate solutions, the cost (number of operations) of using such a method for a system of order n can be up to the order n^3 if A is dense and this is due to the work involved in getting the LU decomposition in the first place. The cost of solving the lower and upper triangular systems can be up to the order n^2 when A is dense. Sometimes an

iterative method may be much more efficient though potentially less accurate.

Now consider the system $Ax = b$ and assume A is non-singular. Let $v \in \mathbb{R}^n$ be an approximation to the solution x. We will denote the error by $e(v) = x - v$ and the residual by $r(v) = b - Av$. Now we need two subspaces, $\mathcal{K}$ and $\mathcal{L}$ of $\mathbb{R}^n$ of the same dimension. We shall try to improve the approximate solution v as in [4, p.402], by a vector w that solves the problem

$$\left\{ \text{Seek } w \in v + \mathcal{K} \text{ such that } r(w) \perp \mathcal{L} \right\}. \tag{2.2.3}$$

Since $\mathcal{K}$ and $\mathcal{L}$ have the same dimension and A is invertible, (2.2.3) is well posed [4]. Choosing $\mathcal{L} = A\mathcal{K}$ we then seek the solution v of (2.2.3) that minimizes the residual $r(v)$ over the space $v + \mathcal{K}$. There are many iterative methods based on the idea of projection. The most commonly used are the conjugate gradient (CG) method and GMRES. CG method applies to systems with symmetric, positive definite matrices and GMRES applies to the general case.

In general, for an iterative projection method we are given $u_0 \in \mathbb{R}^n$; then at the m^{th} step of the iterative process we solve the problem

$$\left\{ \text{Seek } u_m \in u_0 + \mathcal{K}_m \text{ such that } r(u_m) \perp \mathcal{L}_m \right\} \tag{2.2.4}$$

where $\{\mathcal{K}_m\}_{m \geq 1}$ and $\{\mathcal{L}_m\}_{m \geq 1}$ are two sequences of subspaces of $\mathbb{R}^n$.
We next introduce the notion of *Krylov space* since $\mathcal{K}_m$ can be taken as a space of this type. Let $r \in \mathbb{R}^n$, then the space

$$\mathcal{K}(A, r, k) = \text{span}\{r, Ar, \ldots, A^{k-1}r\}$$

is called a Krylov space of order k generated by r and associated with the matrix A. Arnoldi's algorithm is one way of constructing an orthonormal basis for our space

$\mathcal{K}_m$, a Krylov space of order m, associated with the matrix A. The norm $\|\cdot\|_n$ is the Euclidean norm in $\mathbb{R}^n$.

Arnoldi's algorithm

Set $r_0 = b - Au_0$

Set $\beta = \|r_0\|_n$, and $v_1 = r_0/\beta$

set $j = 1$

while $j < m$ do

$h_{i,j} = (Av_j, v_i)_N$ for $i = 1, \ldots, j$

$\widehat{v}_{j+1} = Av_j - \sum_{i=1}^{j} h_{i,j} v_i$

$h_{j+1,j} = \|\widehat{v}_{j+1}\|_n$; if $h_{j+1,j} = 0$ stop

$v_{j+1} = \widehat{v}_{j+1}/h_{j+1,j}$

$j \leftarrow j + 1$

end while

Let us introduce two other matrices, $H_j \in \mathbb{R}^{j+1,j}$ whose ij^{th} entry is the corresponding $h_{i,j}$ from the above algorithm and $V_j \in \mathbb{R}^{n,j}$ whose columns are the first j orthogonal vectors $\{v_1, ..., v_j\}$ generated by the Arnoldi algorithm.

Next we will want to minimize the residual so our problem is to find z such that

$$\min_{z \in \mathcal{K}_m} \|b - A(u_0 + z)\|_n = \min_{z \in \mathcal{K}_m} \|r_0 - Az\|_n$$

We can expand z with respect to the Arnoldi basis $\{v_1, \ldots, v_m\}$ so that $z = V_m y$ for some $y \in \mathbb{R}^m$. Referring to [4, p. 405–407] we see that this problem reduces to the following minimization problem:

$$\min_{y \in \mathbb{R}^m} \|\beta e_1 - H_m y\|_{m+1} \tag{2.2.5}$$

where e_1 is the first vector in the standard basis of $\mathbb{R}^{m+1}$.

This is a Least-Squares problem and the solution is unique [4, p. 406]. To solve it we need to find the QR factorization of the matrix H_m. More details on this process can be found in [4, p. 406]. We now have all the elements to describe the GMRES algorithm.

GMRES Algorithm

Choose u_0 and a tolerance ϵ

Set $m = 0$, $r_0 = b - Au_0$, $\beta = \|r_0\|_n$, and $v_1 = r_0/\beta$

while $\|r_m\|_n > \epsilon$ do

$m \leftarrow m + 1$

$h_{i,m} = (Av_m, v_i)_n$ for $i = 1, \ldots, m$

$\widehat{v}_{m+1} = Av_m - \sum_{i=1}^{m} h_{i,m} v_i$

$h_{m+1,m} = \|\widehat{v}_{m+1}\|$

$v_{m+1} = \widehat{v}_{m+1}/h_{m+1,m}$

Compute the matrix H_m, Q_m and R_m (the QR factorization of H_m),

Compute the vector $g_m = Q_m \beta e_1$

set $\|r_m\|_n = \|g_m\|_n$

end while

solve the system $R_m y = g_m$ where $y = \begin{pmatrix} y_1 \\ \vdots \\ y_m \end{pmatrix}$

set $u_m = u_0 + \sum_{i=1}^{m+1} y_i v_i$

The nice thing about the GMRES algorithm is that it converges in at most n iterations. However, let us recall that the size of the systems of the discretized Navier–Stokes equations can be in the tens or even hundreds of thousands! There are ways to improve the convergence rate of the algorithm without sacrificing a lot of computation time and that is with the help of preconditioners.

2.3 Preconditioning

This section deals with the concept of the *condition number* of a matrix A and its effects on solving the linear system $Ax = b$. In essence, the condition number of a matrix tells you how far away a matrix is from the set of singular matrices. Let us define this so called condition number.

Definition 2.3.1 *Let Z be an invertible $n \times n$ matrix. Its condition number is defined as*

$$\kappa(Z) = \|Z\|_n \|Z^{-1}\|_n.$$

We say that Z is ill-conditioned if $\kappa(Z) \gg 1$.

It can easily be proved as in [4] that the condition number of a matrix is always greater than or equal to 1 and also that when Z is symmetric $\kappa(Z) = \left|\frac{\lambda_{\max}(Z)}{\lambda_{\min}(Z)}\right|$ where $\lambda_{\max}(Z)$ and $\lambda_{\min}(Z)$ are the largest and smallest eigenvalues of Z, respectively. Since we are using numerical methods such as FEM and Newton's method to get to our linear system it is good to see what the effects of perturbation are on the system $Ax = b$. If we look at the system $A(x + \delta x) = b + \delta b$ it is easily shown that

$$\frac{\|\delta x\|_n}{\|x\|_n} \leq \kappa(A) \frac{\|\delta b\|_n}{\|b\|_n},$$

and for the system $(A + \delta A)(x + \delta x) = b$ that

$$\frac{\|\delta x\|_n}{\|x + \delta x\|_n} \leq \kappa(A) \frac{\|\delta A\|_n}{\|A\|_n}.$$

These two estimates tell us that if A is ill-conditioned even slight perturbations in A or b can lead to significant variations of the solution. The idea behind preconditioning a system is to re-write $Ax = b$ as a new linear system $\widetilde{A}\widetilde{x} = \widetilde{b}$ where $\widetilde{A}$ is better conditioned. One way of doing this is to take a non-singular matrix P and split it into the form $P = P_L P_R$ so that the systems $P_L y = a$ and $P_R z = c$ are easy and inexpensive to solve. This P is going to be used as a split-preconditioner:

$$(P_L^{-1} A P_R^{-1})(P_R x) = P_L^{-1} b. \tag{2.3.1}$$

Setting $\widetilde{A} = P_L^{-1}AP_R^{-1}$, $\widetilde{x} = P_R x$ and $\widetilde{b} = P_L^{-1}b$ we have the new system $\widetilde{A}\widetilde{x} = \widetilde{b}$, where $\widetilde{A}$ ideally has a lower condition number then A. This split preconditioner is needed for symmetric matrices involving methods like CG in order to preserve the symmetry of $\tilde{A}$ but due to the fact that GMRES works for non-symmetric $\tilde{A}$, it is more convenient and useful to simply use a left preconditioner or right preconditioner. Let us consider a left preconditioned GMRES. The associated Krylov space would then be

$$\mathcal{K}_m^P = \text{span}\{r_0, (P^{-1})Ar_0, \ldots, (P^{-1}A)^{m-1}r_0\}.$$

Now by replacing A by $P^{-1}A$ and b by $P^{-1}b$ we can obtain a new preconditioned algorithm for GMRES that would have a faster convergence rate than the original.

There are many ways you can precondition a linear system. Some of the more common preconditioners include the Incomplete LU factorization (ILU), Successive Over-Relaxation (SOR) and Jacobi. Here we shall briefly explain the ILU, Jacobi and block Jacobi preconditioners since we found these to be the most effective among those tested while requiring a limited amount of memory to solve the Navier–Stokes equations.

The basic idea of ILU is to form a simplified version of the LU factorization of the matrix A, hence the name Incomplete LU factorization. If we are working with the preconditioned system $P^{-1}Ax = P^{-1}b$ where P is the preconditioning matrix, we will want to form upper and lower triangular matrices, $\mathcal{L}$ and $\mathcal{U}$, from A while maintaining the sparsity pattern of A. That is, if the ij^{th} entry of A is 0 then the ij^{th} entry of the matrix $P = \mathcal{L}\mathcal{U}$ is also 0. The algorithm below is the basic scheme for an ILU factorization and can also be found in [4, p. 413]. In Saad [12, p. 275] this algorithm is also described in more detail and the author goes a step further to explain different levels of filling. The algorithm below is known as ILU(0) since it has no levels of extra

filling. The ILU(1) factorization has one level of filling and results from taking P to be the zero pattern of the product $\mathcal{LU}$ of the factors $\mathcal{L}$ and $\mathcal{U}$ obtained from ILU(0). For further levels of fill see [12].

ILU(0) Factorization Algorithm

for $i = 2, ..., n$ do
  for $k = 1, ..., i-1$ do
    if $A_{ik} \neq 0$ then
      $A_{ik} \leftarrow A_{ik}/A_{kk}$
      for $j = k+1, ..., n$ do
        if $A_{ij} \neq 0$ then
          $A_{ij} \leftarrow A_{ij} - A_{ik}A_{kj}$
        end if
      end or
    end if
  end for
end for

The Jacobi preconditioner is one of the simplest ones; it is simply a diagonal matrix whose elements are precisely those of the matrix of the system in question. For the system $P^{-1}Ax = P^{-1}b$, $P = D$ where D is the diagonal matrix just described. The block Jacobi preconditioner is a block diagonal matrix and in the PETSC documentation [1] it uses the ILU method to fill in each individual block and the blocks themselves can be taken to be of any size desired.

2.4 Portable, Extensible Toolkit for Scientific Computation (PETSC)

PETSC is a suite of data structures and routines adapted for calculations of solutions of partial differential equations. It is intended for large-scale projects and features many libraries providing linear and nonlinear equations solvers that can be used in conjunction with C, C++, Fortran and Python [1]. PETSC provides routines for solving the linear and nonlinear components of an algebraic differential equation like the one derived in (1.2.2). The Scalable Nonlinear Equations solver (SNES) gives the user access to Newton-based methods for solving nonlinear algebraic differential equations such as equation (1.2.2) derived in section 1.2. Once the equation has been linearized via the SNES the scalable linear equations solver (KSP) will provide Krylov subspace based iterative methods. It is within these two interfaces that the user can specify the type of iterative solver and precondtioners to use. A useful linear solver provided by KSP is the Generalized Minimal Residual (GMRES) method. It is appropriate for large sparse matrices that are non-symmetric as in the case of the discretized Navier–Stokes equations. KSP also offers many choices for a preconditioner. The list of available preconditioners includes Jacobi, Block Jacobi, ILU, ILU(n) and Successive Over-Relaxation (SOR). Among the many types of convergence tests PETSC offers, there are three in particular used for the SNES and KSP solvers, stol, atol and rtol. One can declare convergence when the norm of the change in the solution between successive iterations is less then some tolerance, stol. The tolerance atol is the absolute size of the norm and rtol is the relative decrease of the absolute size of the norm. It is also possible to bypass these convergence tests and specify a given number of Newton or linear solver iterations.

Chapter 3

Comparison of Iterative Methods

In this chapter we will compare the performance of the iterative solver GMRES used with preconditioners presented in Chapter 2 using three test cases:

i) a 2D steady lid-driven cavity

ii) a 2D pulsating lid-driven cavity

iii) a 3D steady lid-driven cavity.

3.1 Results for a 2D Steady Lid-driven Cavity

In this section I will present several results obtained on a simple 2D square lid-driven cavity. This is a well-documented case and the benchmark solution used for comparison will be that of Ghia and Ghia [5]. Let us first discuss the domain of the test case. It is the unit square cavity $(0,1) \times (0,1)$ with upper horizontal boundary called the lid which is put into motion using the boundary condition $u(x,1,t) = (U(t),0)$ where $U(t)$ is a prescribed function. For the steady lid-driven case $U(t) = 1$. All other sides of the cavity (walls) are set to have a no-slip boundary condition which means that $u = 0$ on the walls. The characteristic length and velocity are $L = 1$ and $V = 1$,

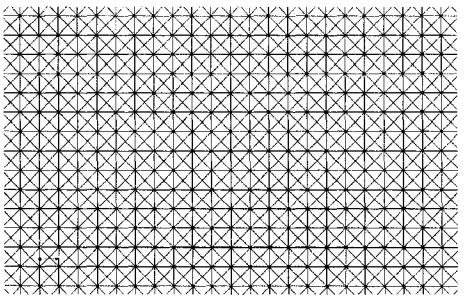

Figure 3.1: A close up of the mesh in 2 dimensions

respectively which yields a Reynolds number of simply $\mathrm{Re} = 1/\nu$. Let us discuss the size of the mesh. The mesh size is determined in the following way: in 2D, the square is divided into a square grid of, say, $N \times N$ and then each square formed by this is cut into 4 triangles (by connecting the diagonals), hence denoting its mesh size by $N \times N \times 4$. In figure 3.1 we can see a close-up of the 2-dimensional mesh. Another parameter up for discussion is the size of the timestep to take. For the first test case of a $100 \times 100 \times 4$ mesh with $\mathrm{Re} = 100$, a step size of $1, 10, 50$ and 100 will be tried in order to reach the final time of $t = 100$. Based on the results from this case we shall determine what is the optimal size to use for larger and more complicated test cases. The goal will always be to reach optimum accuracy while maintaining a CPU time comparative, if not better, to that of the direct LU factorization method since it is more commonly used and known to be reliable.

Before getting into the numerical results we will take a look at some published results on similar test cases. Presented in a paper by Ghia and Ghia [5] are some visual 2D results on the same problem we are studying that can help confirm any results obtained with an iterative method. We can use the LU factorization method as a basis for comparison since its accuracy is reliable. In figure 3.2 (a) is Ghia and Ghia's [5] result on a 2D steady lid-driven cavity with Reynolds number of 100 and (b) the same 2D lid-driven cavity is presented whose results were obtained using the LU fac-

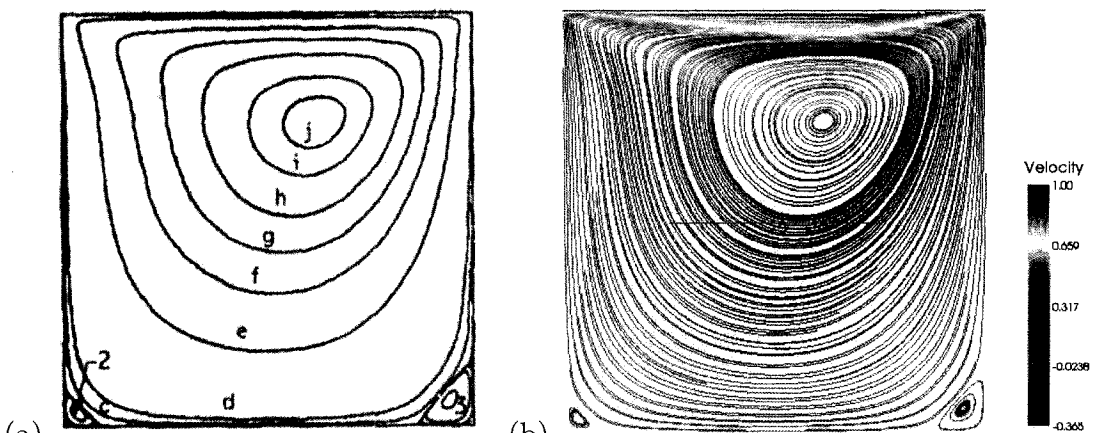

(a) (b)

Figure 3.2: Steady lid-driven cavity with Re = 100 from (a) Ghia and Ghia [5] and (b) using LU factorization in PETSC.

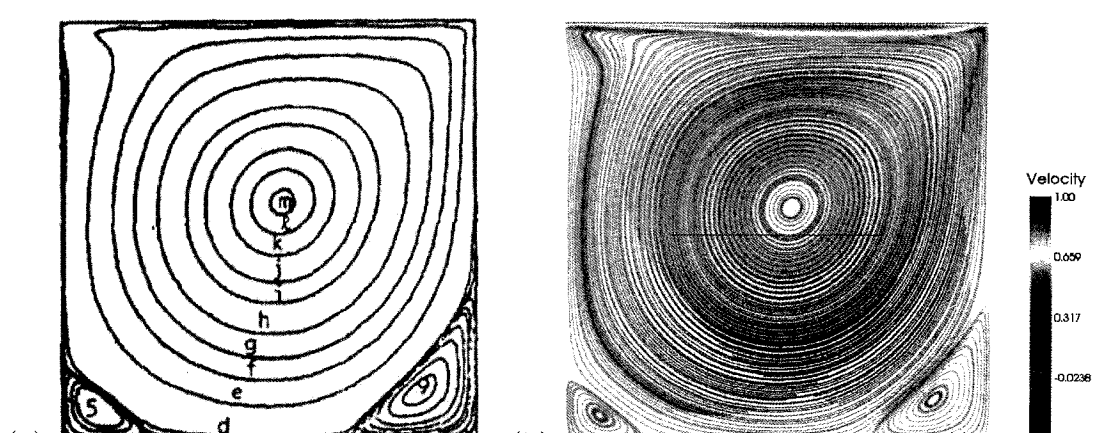

(a) (b)

Figure 3.3: Steady lid-driven cavity with Re = 1000 from (a) Ghia and Ghia [5] and (b) using LU factorization in PETSC.

torization in PETSC. Similarly in figure 3.3(a) is Ghia and Ghia's result on a 2D steady lid-driven cavity with Reynolds number of 1000 and (b) the results obtained with the LU factorization in PETSC.

When experimenting with solvers it is good to look at the locations of vortices and the prominent curves in the streamlines in order to have a good idea how well the solvers are working. At a Reynolds number of 100 we see that the two vortices in the bottom corners are much smaller than those of the case when the Reynolds number is 1000. Also the location of the main vortex near the center is higher and to the right at Re = 100 and at Re = 1000 it is moving its way closer to the center. One other thing to note is the curve in the streamlines going towards the top left corner. The lid of the cavity is moving in the positive x-direction and so this is pushing the streamlines and forcing them to have a slight curve that becomes more evident in the Re = 1000 case, as in agreement with remarks from Ghia and Ghia [5].

Now let us look at the numerical results on the 2D steady lid-driven test case with the iterative solver GMRES. The options that are going to be varied in the test cases are the types of preconditioners (PC type) used, the number of linear iterations (KSPits), the number of nonlinear iterations (SNESits) and the stepsize. The CPU time, memory used and the norm of the residuals (KSPres and SNESres) at the final timestep are recorded at the end of each trial. A summary of this data for a test case with mesh size $100 \times 100 \times 4$ and Reynolds number Re = 100 is given in table 3.1. The first line shows the efficiency of the LU factorization. We can see that it yields high accuracy using only about 5 minutes of CPU time; however, it is the method that requires the largest amount of memory at 199 Mb. The total number of Newton iterations required for this test case was 20 as we allowed PETSC to use its default stopping criteria so that each timestep yields a different number of iterations depending on the norms of the linear and nonlinear residuals. The default relative

tolerance for the SNES iterations in PETSC is 1×10^{-08}. This means that when the ratio of two consecutive Newton iterations becomes equal to or smaller than this tolerance, we shall stop the iteration process. In this first case the average number of Newton iterations required to perform the LU factorization was about 4 per timestep.

When applying the iterative methods we started by using the preconditioner with the smallest memory requirement, the Jacobi preconditioner. It only requires about 49 Mb of memory; however it yields poor results and the norms of the residuals are not small enough to obtain a solution similar to Ghia's or that of the LU factorization. The Block Jacobi and the ILU(0) worked at the same efficiency. This is because the Block Jacobi preconditioner uses ILU(0) to fill its entries at the block level. In all following test cases, Block Jacobi will be excluded as it yields identical results to that of ILU(0). When using ILU(0) we can see that the memory required to store the systems of equations has grown to about 65 Mb. Figure 3.4 shows the pictures for the four tests from table 3.1 that have a †. We want to be able to see how the results compare to (a) LU factorization so in figure (b) we have the case when ILU(0) is used with 30 KSPits and 10 SNESits since we finally obtained a result that is comparable in CPU time to that of LU factorization taking only 12 minutes to resolve (LU took only 5 minutes). In (c) we have the case when ILU(1) is used with 30 KSPits and 5 SNESits are used. The memory is getting higher for this case using up 81Mb but is still significantly lower than the 199 Mb required for LU. The residuals are getting smaller with this preconditioner and since fewer SNESits were required to perform the calculations, the CPU time diminished from that of the ILU(0) case to about 7.2 minutes. The last figure (d) is the result obtained with the ILU(2) preconditioner. This one requires 110 Mb of memory but yields the smallest residuals of all the other preconditioners tried.

Since we have found that the iterative method GMRES on the $100 \times 100 \times 4$ cav-

PC type	KSPits	SNESits	KSPres	SNESres	Mem(Mb)	CPU(min)
LU†	30	20 total	6.08×10^{-20}	1.64×10^{-14}	199	5.0
Jacobi	30	50	2.56×10^{-01}	4.18×10^{-03}	49	54
Jacobi	30	25	2.56×10^{-01}	4.18×10^{-03}	49	27
BJacobi	30	50	1.61×10^{-05}	1.86×10^{-08}	65	59
BJacobi	30	25	1.48×10^{-03}	5.52×10^{-05}	65	30
ILU(0)	30	50	1.61×10^{-05}	1.86×10^{-08}	65	59
ILU(0)	30	25	1.48×10^{-03}	5.52×10^{-05}	65	29
ILU(0)†	30	10	2.49×10^{-02}	7.21×10^{-04}	65	12
ILU(1)	30	50	1.76×10^{-05}	1.70×10^{-08}	81	66
ILU(1)	30	25	1.68×10^{-05}	2.35×10^{-08}	81	33
ILU(1)	30	10	4.54×10^{-05}	8.03×10^{-08}	81	14
ILU(1)†	30	5	6.13×10^{-05}	7.15×10^{-07}	81	7.2
ILU(1)	100	5	5.79×10^{-05}	8.28×10^{-08}	81	9.0
ILU(2)†	100	5	1.76×10^{-05}	2.67×10^{-08}	110	13

Table 3.1: Numerical results for cavity size 100 × 100 × 4 with 10 timesteps of size 10 and Re = 100. Each uses GMRES except LU factorization.

ity with Reynolds number of 100 were accurate enough with ILU(1) and ILU(2) to yield satisfactory visual results, our next task is to see how they measure up when we increase the stepsize. The solution is steady for this test case, so by varying the stepsize we may be able to decrease the CPU time even more. Table 3.2 shows numerical results of this. The LU factorization is capable of doing calculations with 2 timesteps of size 50, yielding the result in figure 3.5 (a). For this test, the number of SNESits required before the stopping criteria is met is just 5 for the first timestep and than 4 for the second timestep. Again increasing the stepsize to 100 and using only one timestep we see in figure 3.5 (b) that the LU factorization is still giving accurate results. The preconditioners ILU(1) and ILU(2) both were useful when 2 timesteps of size 50 were used, see figure 3.6 for the test cases marked with †, but did not even compare to the LU factorization method at just 1 timestep of size 100.

Next we applied similar types of iterative methods to the 2D lid-driven cavity with

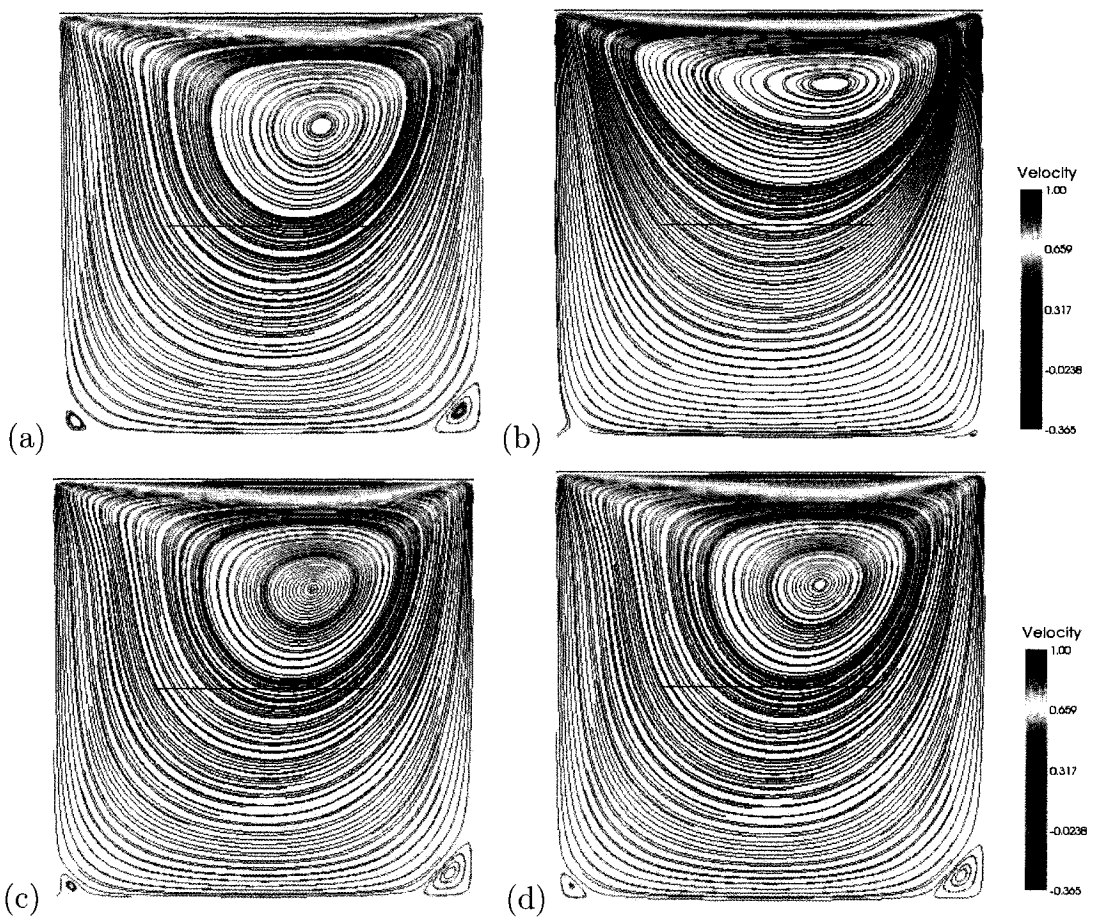

Figure 3.4: The meshsize is $100 \times 100 \times 4$, the stepsize is 10, the number of timesteps is 10 and $Re = 100$. LU factorization is used for (a). The iterative solver GMRES is used with (b) ILU(0), 30 KSPits and 10 SNESits, (c) ILU(1), 30 KSPits and 5 SNESits, (d) ILU(2), 100 KSPits and 5 SNESits.

PC type	stepsize	KSPits	SNESits	KSPres	SNESres	Mem(Mb)	CPU(min)
LU	50	30	5, 4	2.73×10^{-21}	1.37×10^{-16}	199	2.0
ILU(1)	50	100	5	1.25×10^{-03}	1.24×10^{-04}	81	1.8
ILU(1)†	50	100	10	8.36×10^{-05}	7.25×10^{-05}	81	3.7
ILU(1)	50	100	25	5.80×10^{-05}	7.19×10^{-05}	81	9.3
ILU(2)†	50	100	10	7.71×10^{-05}	7.19×10^{-05}	110	4.4
LU	100	30	5	6.54×10^{-21}	1.37×10^{-16}	199	1.2
ILU(1)	100	100	10	7.22×10^{-04}	2.00×10^{-01}	81	1.9
ILU(1)	100	100	50	4.75×10^{-05}	2.00×10^{-01}	81	9.0
ILU(2)	100	100	10	1.17×10^{-04}	2.00×10^{-01}	110	2.3

Table 3.2: Numerical results for cavity size $100 \times 100 \times 4$ with 2 timesteps of size 50, 1 timestep of size 100 and Re = 100. Each uses GMRES except LU factorization.

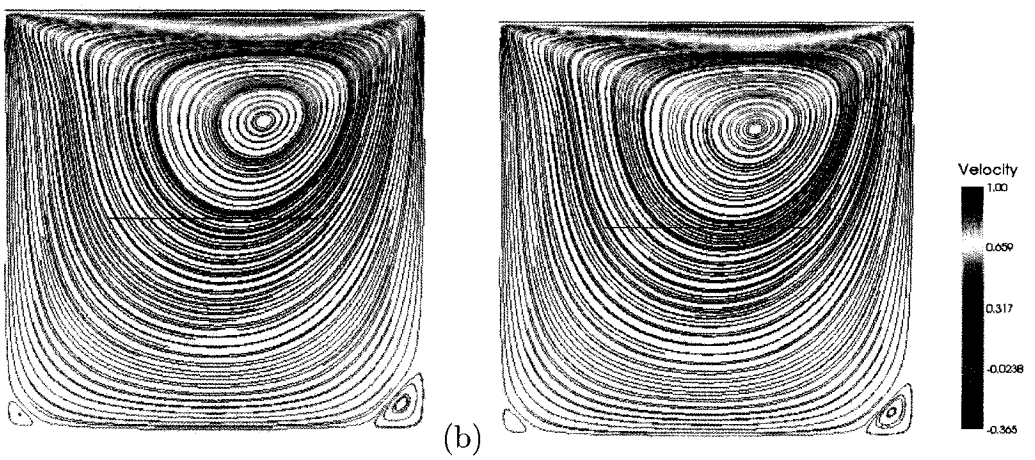

Figure 3.5: The meshsize is $100 \times 100 \times 4$ with Re = 100 using LU factorization with a stepsize of 50 in (a) and a stepsize of 100 in (b)

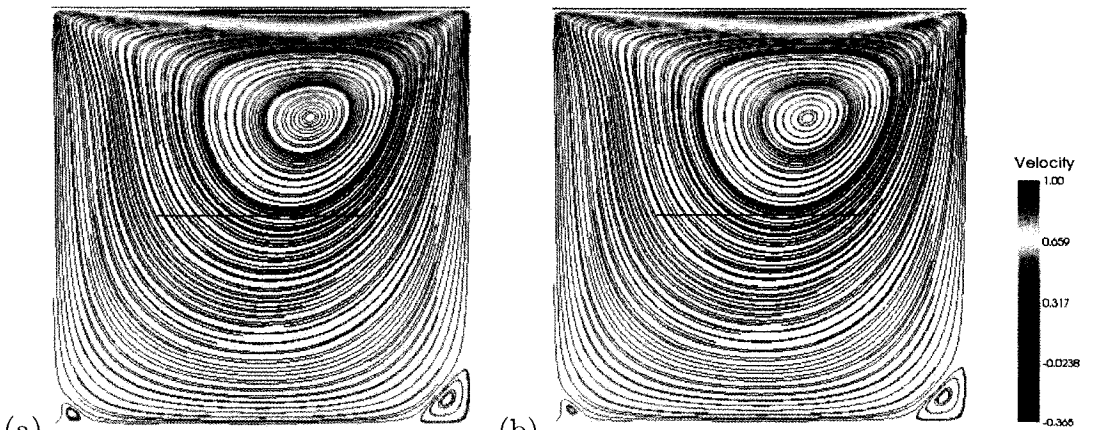

Figure 3.6: The meshsize is $100 \times 100 \times 4$ with Re = 100 using GMRES, 100 KSPits and 10 SNESits, a stepsize of 50 and with preconditioners (a) ILU(1) and (b) ILU(2).

a Reynolds number of 1000, the optimum solution being one that most resembles that in figure 3.3(a), our known result. The direct LU factorization method was first applied to a mesh size $100 \times 100 \times 4$ to gain knowledge on the CPU time and memory requirements for this test case. We see in table 3.3 that the LU factorization requires about 199 Mb of memory, takes a total of 32 Newton iterations and needs about 8 minutes to run the simulation. Using the iterative method GMRES we once again obtain several more numerical results. Looking at Ghia's result in figure 3.3(a) we see that figure 3.3(b) obtained with LU factorization is once again a reliable solution. When using the presonditioned GRMES we obtain similar results as in the case when Re = 100. The best result was obtained using ILU(2) as a preconditioner with 100 KSPits and 5 SNESits. This trial required about 110 Mb of memory and about 11 minutes of CPU time. We have succeeded in reducing the memory requirement to about 55% of what was needed for the LU factorization. It is possible to obtain a reasonable result even with ILU(0), which utilized about 65 Mb of memory. This is about 32% of the memory required for LU factorization. The major dissimilarity in this result is in the bottom left corner. In Figure 3.7 (a) we have the reference

PC type	KSPits	SNESits	KSPres	SNESres	Mem(Mb)	CPU(min)
LU†	30	32 total	1.61×10^{-22}	3.10×10^{-17}	199	8.1
ILU(0)	30	25	7.30×10^{-05}	6.40×10^{-07}	65	30
ILU(0)†	30	10	8.29×10^{-05}	7.37×10^{-07}	65	12
ILU(1)	30	25	1.52×10^{-04}	5.51×10^{-07}	81	34
ILU(1)	30	10	2.37×10^{-04}	7.74×10^{-07}	81	13
ILU(1)	100	5	2.24×10^{-04}	7.54×10^{-07}	81	10.9
ILU(2)†	100	5	5.00×10^{-06}	1.98×10^{-07}	110	11.1

Table 3.3: Numerical results for cavity size $100 \times 100 \times 4$ with 10 timesteps of size 10 and Re = 1000. Each uses GMRES except LU factorization.

solution obtained with LU factorization. In 3.7(b) one can see what was obtained using the ILU(0) preconditioner with GMRES. The lower left corner of this picture is the only obvious discrepancy from the reference solution. In 3.7 (c) is the case when ILU(2) was used and one can see that this one is very close to our reference solution and to Ghia's results. These three results are the ones in table 3.3 that are marked with a †.

Refining the mesh to a $200 \times 200 \times 4$ gives similar results. One can see in figure 3.8 (a) a result for direct LU factorization which required a total of 32 Newton iteration, 913 Mb of memory and needed 37 minutes of CPU time. The data from table 3.4 show that iterative methods only become accurate enough once we use higher levels of fill with the ILU preconditioner, which ultimately is just making the method closer to the direct LU method, also adding to the CPU time. The three test cases in fig 3.8 are marked with a † in table 3.4. In 3.8(a) is our reference solution using LU factorization with 10 timesteps and the stopping criteria prescribed in PETSC. The number of SNESits is said to be varying* since it is not a constant number at each timestep. The total number of Newton iterations calculated for the LU factorization test case was 19 and the CPU time was about 37 minutes. In figure 3.8(b) we have the test case using preconditioned GMRES with ILU(1), 30 KSPits and 5 SNESits.

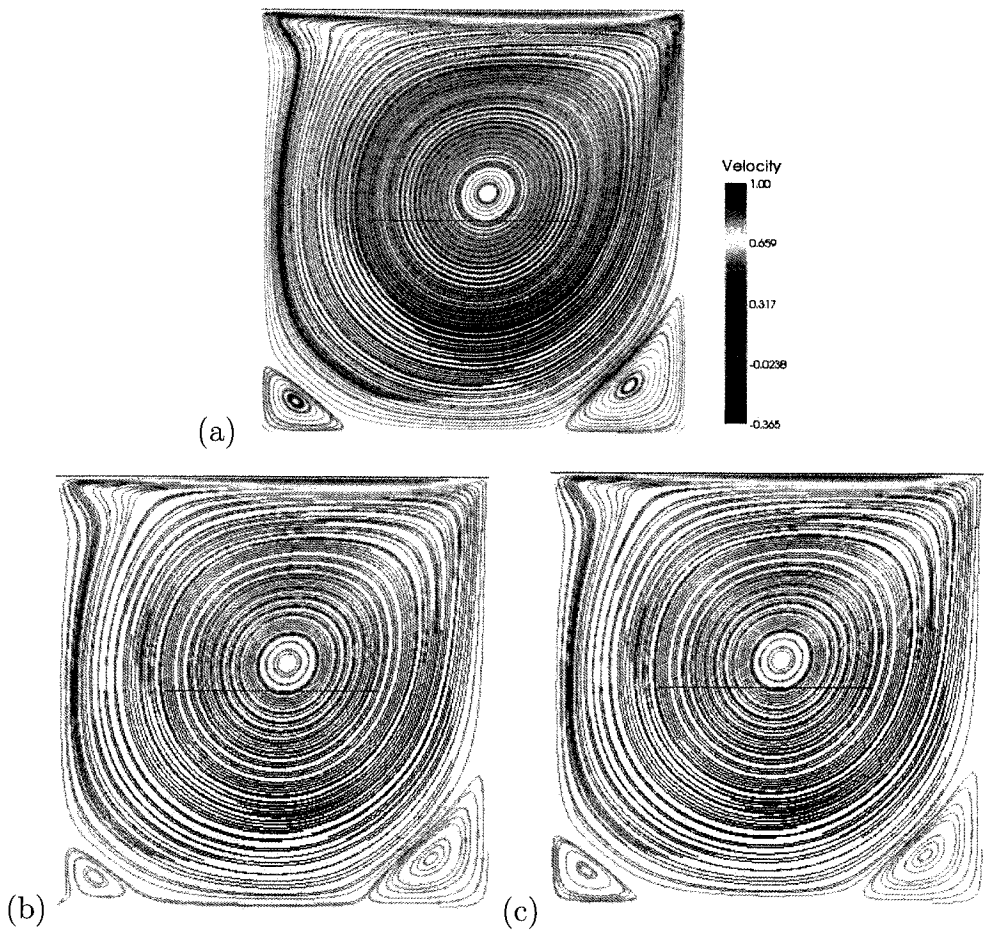

Figure 3.7: The meshsize is $100 \times 100 \times 4$, the stepsize is 10, the number of timesteps is 10 and Re = 1000. LU factorization is used to obtain (a). ILU(0) with 30 KSPits and 10 SNESits is used for (b). ILU(2) with 100 KSPits and 5 SNESits is used for (c).

PC type	KSPits	SNESits	KSPres	SNESres	Mem(Mb)	CPU(min)
LU†	30	19 total	8.69×10^{-19}	8.77×10^{-15}	913	37
ILU(0)	30	25	3.80×10^{-01}	3.74×10^{-03}	235	201
ILU(0)	30	10	3.80×10^{-01}	3.74×10^{-03}	235	81
ILU(1)	30	25	2.74×10^{-03}	2.34×10^{-05}	313	255
ILU(1)	30	10	1.75×10^{-03}	2.44×10^{-05}	313	102
ILU(1)†	30	5	8.63×10^{-03}	8.10×10^{-05}	313	43
ILU(1)	100	5	1.11×10^{-03}	9.67×10^{-06}	313	54
ILU(2)†	100	5	4.47×10^{-05}	1.21×10^{-07}	426	70

Table 3.4: Numerical results for cavity size 200 × 200 × 4 with 10 timesteps of size 10 and Re = 100. Each uses GMRES except LU factorization.

This test case is here since the CPU time to achieve the result was about 43 minutes, close to the 37 minutes required for the LU factorization, however a closer look at the picture shows that the shape of the vortex is slightly flatter than the solution obtained with LU. Next we used the GMRES precondioned with ILU(2) which by figure 3.8 shows a nearly identical result to that of LU factorization but with a CPU time of about 70 minutes, almost double that of LU factorization. The memory requirement for ILU(2) was about 426 Mb which is less then half of what was needed for LU. If we wish to conserve CPU time, LU factorization is more timely but if we wish to conserve memory than the iterative solver GMRES with ILU(2) is the more appropriate choice.

Still using the mesh size 200 × 200 × 4 we increased the Reynolds number to 1000. In this case the LU factorization method creates a zero pivot column causing the iterative method to stop. The memory required to fill the matrices of the systems of equations was still obtainable and was about 913 Mb. The iterative solver GMRES was then tested and ILU(1) with 100 KSPits and 5 SNESits gave a satisfactory result, both in terms of accuracy of the solution and CPU time. It is marked by a † in table 3.5 and displayed in figure 3.9(a). When ILU(2) was used to precondition GMRES it did not make a significant difference in the solution, as we can see by looking at the

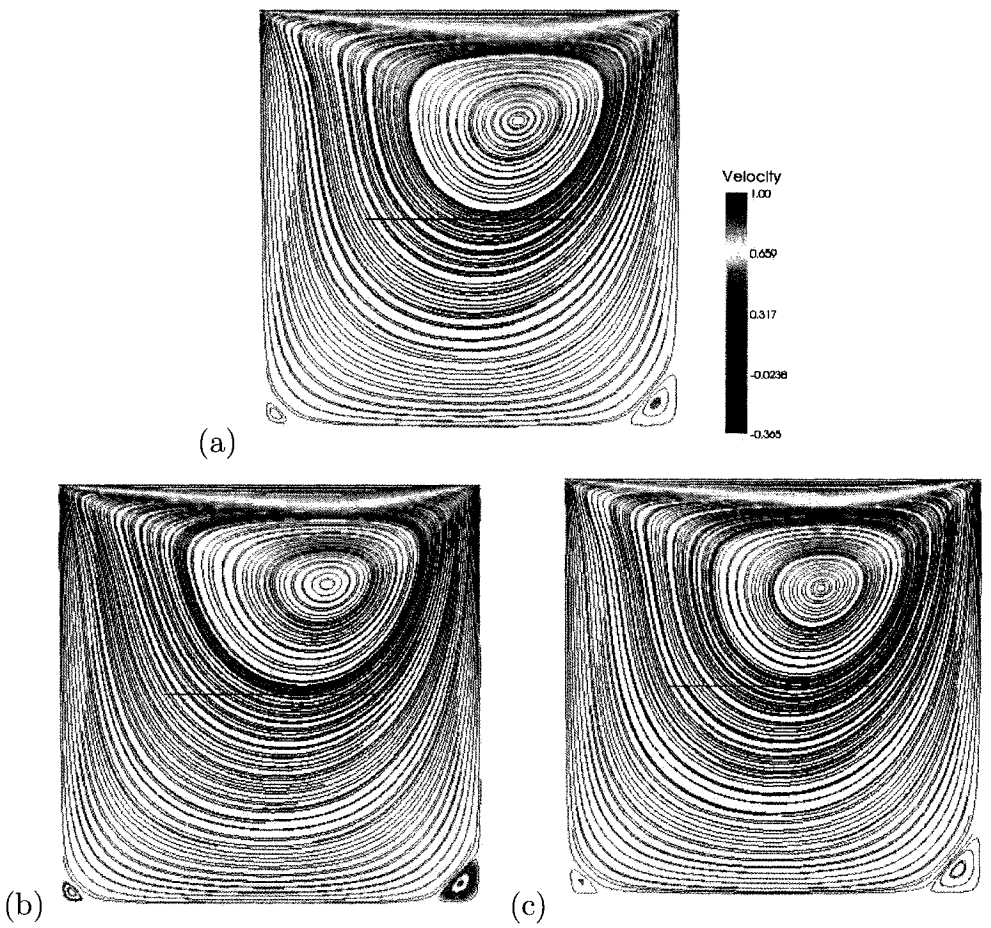

Figure 3.8: The meshsize is 200 × 200 × 4, the stepsize is 10, the number of timesteps is 10 and Re = 100. LU factorization is used for (a). The iterative solver GMRES is used with ILU(1), 30 KSPits and 5 SNESits in (b). ILU(2) with 100 KSPits and 5 SNESits is used for (c)

PC type	KSPits	SNESits	KSPres	SNESres	Mem(Mb)	CPU(min)
LU	30	–	–	–	913	–
ILU(0)	30	10	8.25×10^{-03}	4.04×10^{-05}	313	78
ILU(1)	30	10	1.40×10^{-04}	1.68×10^{-07}	313	97
ILU(1)†	100	5	1.52×10^{-04}	1.41×10^{-07}	313	53
ILU(2)†	100	5	2.92×10^{-04}	1.32×10^{-07}	426	61

Table 3.5: Numerical results for cavity size $200 \times 200 \times 4$ with 10 timesteps of size 10 and Re = 1000. Each uses GMRES except LU factorization.

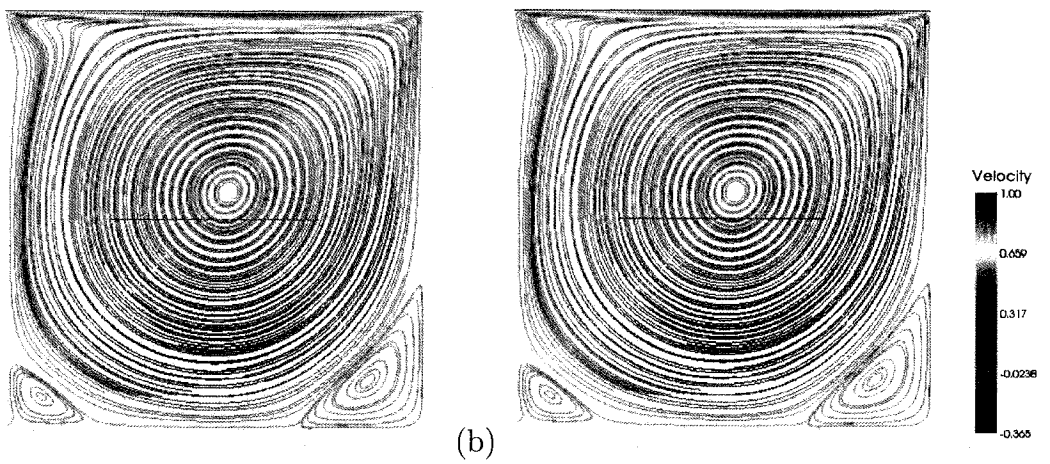

Figure 3.9: The meshsize is $200 \times 200 \times 4$, the stepsize is 10, the number of timesteps is 10 and Re = 1000. The iterative solver GMRES is used with ILU(1), 100 KSPits and 5 SNESits for (a) and GMRES with ILU(2), 100 KSPits and 5 SNESits is used for (b).

size of the residuals for these two methods and from figure 3.9 (b) where the solution is practically identical to that of ILU(1).

At a mesh of $400 \times 400 \times 4$ elements on the 2D cavity we see in table 3.6 that, with the 8 gigabytes of memory available for calculations, the direct LU method was not able to perform. One way to fix this problem would be to do parallel computing, which means to have different processors doing separate parts of the job at the same time, splitting the memory requirements on the nodes of a cluster. A few tests using GMRES were done on this meshsize, however with a stepsize of 10 the residuals were

PC type	stepsize	KSPits	SNESits	KSPres	SNESres	Mem(Mb)	CPU(min)
LU	10	–	–	–	–	–	–
ILU(0)	10	30	10	8.00×10^{-01}	3.34×10^{-03}	926	671
ILU(1)	10	30	10	$1.29 \times 10^{+00}$	2.84×10^{-03}	1226	599
ILU(1)	10	100	5	4.09×10^{-01}	1.19×10^{-03}	1226	366
ILU(1)	5	100	5	3.56×10^{-01}	1.18×10^{-03}	1226	780
ILU(2)	10	100	5	1.85×10^{-02}	5.48×10^{-05}	1697	427
ILU(2)†	5	100	5	3.27×10^{-05}	5.57×10^{-08}	1697	840

Table 3.6: Numerical results for cavity size $400 \times 400 \times 4$ and Re $= 100$.

not small enough to obtain nice results, hence reducing the stepsize to 5 was necessary for some of the test cases. Reducing the stepsize from 10 to 5 with the ILU(1) preconditioner did not help our situation as the residuals of the linear and nonlinear systems stayed at the same order of $O(10^{-1})$ and $O(10^{-5})$, respectively. When ILU(2) was used the difference was more significant upon reducing the stepsize. The CPU time for ILU(2) with 100 KSPits, 5 SNESits and stepsize of 5 was about 840 minutes (14 hours). The simulation of this case can be found in figure 3.10 (b). Since we could not obtain results for the LU method for this meshsize, Ghia's result is put next to ours in figure 3.10 (a). In table 3.6 we can see which test cases were tried in PETSc and the one marked with a † is the one in figure 3.10 (b). This strategy of reducing the stepsize was successful as the result was accurate enough to generate nearly identical streamlines as that in Ghia's result for Re $= 100$.

Now that we have some numerical results for three mesh sizes for the steady lid-driven cavity, it is worth noting the scaling of the CPU time and memory between the three. Let us first observe what the ratios between memory requirement of the LU factorization method with Re $= 100$. At $100 \times 100 \times 4$ the memory required to perform the calculations is about 199 Mb, at $200 \times 200 \times 4$ it needs about 913 Mb and at $400 \times 400 \times 4$ we were unable to do this calculation since it required more than the 8 Gb of memory we had available for doing computations. This indicates a growth of

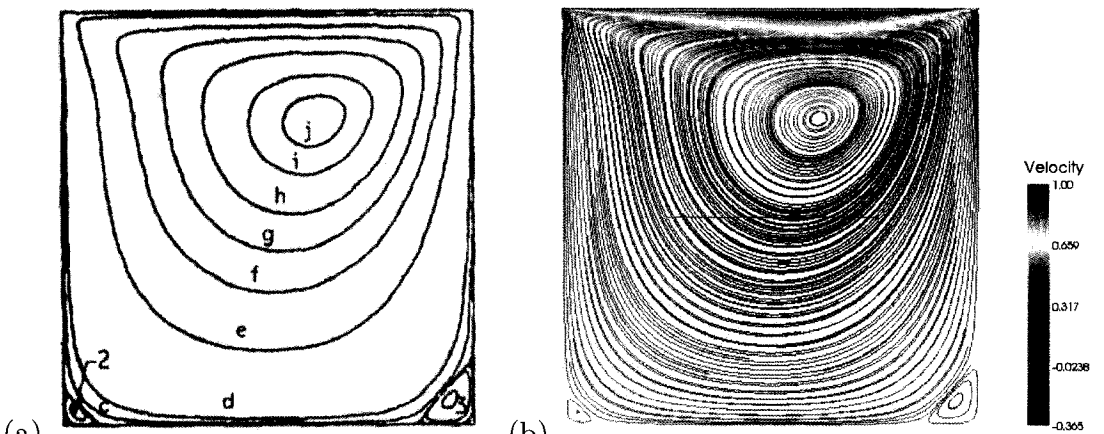

Figure 3.10: (a)Result obtained on a steady lid-driven cavity obtained by Ghia [5]. (b) The meshsize is 400 × 400 × 4, the stepsize is 5, the number of timesteps is 20 and $Re = 100$. The iterative solver GMRES is used with ILU(1), 100 KSPits and 5 SNESits.

memory requirement that is at least superlinear for the direct method. For ILU(0), ILU(1) and ILU(2) the ratio for memory requirement between the 100 × 100 × 4 and 200 × 200 × 4 cavities is about 3.7 . The ratio between the 200 × 200 × 4 and 400 × 400 × 4 cavities is about 3.9 for ILU(2) and ILU(1) (ILU(0) was not tested for the 400 × 400 × 4 cavity). By doubling the number of grid points in each direction, the mesh size is multiplied by four. From the result obtained, asymptotic growth rate of memory for GMRES preconditioned with ILU(k) might very well be four, i.e. a linear growth rate of memory requirement. Figure 3.11 shows a graph of the memory requirements for the four methods discussed against the number of unknowns which is calculated using $3((N+1)^2+N^2)$ for an $N \times N \times 4$ mesh. The horizontal axis is the number of unknowns and the vertical axis is the memory required. The data from this graph is obtained from table 3.7 which summarizes the memory requirements from all of our relevant test cases.

The following figure 3.12 shows the CPU time per Newton iteration of the LU factor-

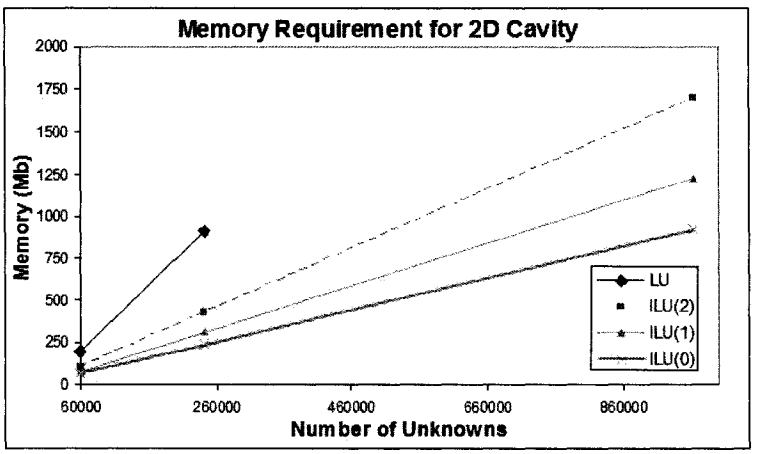

Figure 3.11: The memory requirements for the preconditioned GMRES using ILU(0), ILU(1), ILU(2) and LU factorization versus the number of unknkowns for cavity sizes $100 \times 100 \times 4$, $200 \times 200 \times 4$ and $400 \times 400 \times 4$ and Re $= 100$.

N	# of unknowns	LU	ILU(2)	ILU(1)	ILU(0)
100	60603	199	110	81	65
200	241203	913	426	313	235
400	962403	> 8000	1697	1226	926

Table 3.7: Memory requirements in Mb for cavity size $N \times N \times 4$, Re $= 100$.

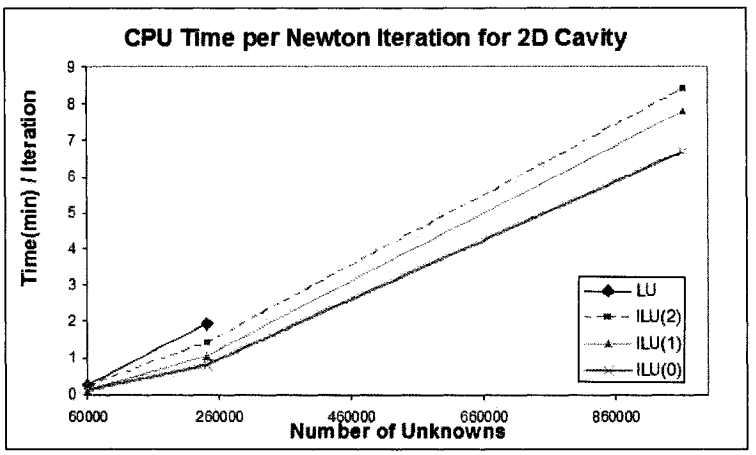

Figure 3.12: The CPU time per Newton iteration versus the number of unknowns required for the preconditioned GMRES using ILU(0), ILU(1), ILU(2) and LU factorization for cavity sizes $100 \times 100 \times 4$, $200 \times 200 \times 4$ and $400 \times 400 \times 4$ and Re $= 100$.

N	# of unkowns	LU	ILU(2)	ILU(1)	ILU(0)
100	60603	0.26	0.26	0.13	0.12
200	241203	1.95	1.40	1.08	0.81
400	962403	–	8.40	7.80	6.71

Table 3.8: CPU Time per Newton Iteration (minutes per iteration) for cavity size $N \times N \times 4$ of some of the best results for Re $= 100$.

ization and the preconditioned GMRES using ILU(0), ILU(1) and ILU(2). In order to obtain this data, the total CPU time of a test case using was divided by the total number of SNESits. The number of unknowns is along the horizontal axis and the time in minutes per iteration is along the vertical axis. LU factorization is the method requiring the most time per Newton iteration and the most economical in this sense, was GMRES with the preconditioner ILU(0). Table 3.8 summarize the data used to obtain the figure.

The graph 3.13 shows the total CPU time for some of the best results obtained in this sectin. Table 3.9 summarizes these CPU times. We can see that for each precondi-

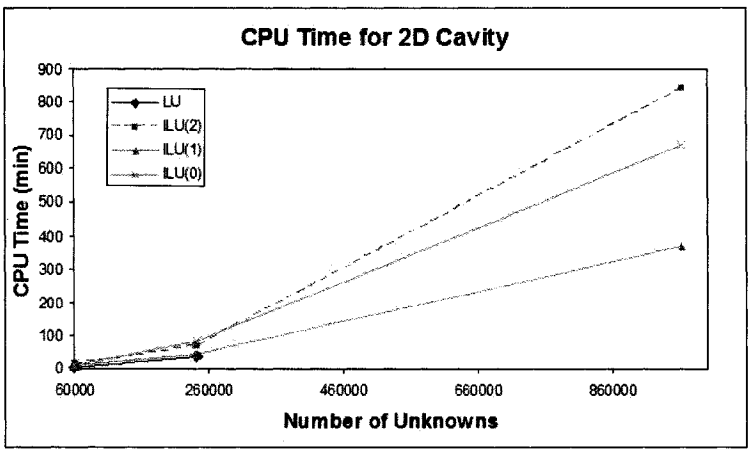

Figure 3.13: The total CPU time versus the number of unknowns of the best results from the preconditioned GMRES using ILU(0), ILU(1), ILU(2) and LU factorization for cavity sizes $100 \times 100 \times 4$, $200 \times 200 \times 4$ and $400 \times 400 \times 4$ and Re = 100.

N	# of unknowns	LU	ILU(2)	ILU(1)	ILU(0)
100	60603	5	13	7.2	12
200	241203	37	70	43	81
400	962403	–	840	780	671

Table 3.9: Total CPU Time (min) for cavity size $N \times N \times 4$ of some of the best results for Re = 100

tioned GMRES trial we were able to obtain a result in an amount of time comparable to that of the LU factorization.

The data obtained from the numerical solutions contains the norms of the nonlinear residuals at each time step. A further analysis of this information allows us to compare how each method, the direct and the iterative solver, converges at each timestep. By taking each nonlinear residual from the Newton iterations, figure 3.14 was constructed in a cumulative way so that each peak represents the residual of the first iteration and each crevasse represents the residual of the final iteration. It is clear that the direct LU factorization produces a much faster convergence resulting in the significantly

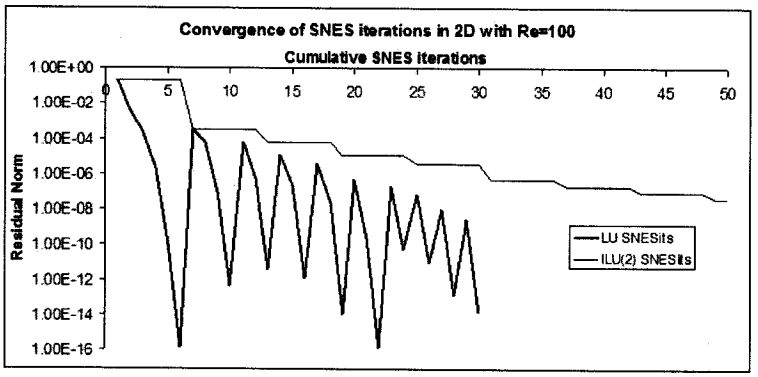

Figure 3.14: The cumulative Newton steps residuals over 10 timesteps for the 2D solvers

lower residuals. The iterative solver also has a converging residual but we see that it converges at a slower rate and the final residual are not getting smaller after each step.

For all of the 2D test cases, it was always beneficial to reduce the stepsizes when using the iterative methods since this always lead to more accurate results, however by reducing the stepsize we increase the CPU time. The CPU time was an important factor in this research since we want to ultimately find an iterative method that would at the very least match that of the direct LU method. This was not the case in the 2D test cases.

3.2 Results for a 3D Steady Lid-driven Cavity

We will now present several results obtained on a 3D cube lid-driven cavity. This test case has been documented in a paper by P. Shankar and M. Deshpande [13] and their results will be used for comparison purposes. Shankar's paper shows results for the 3D steady lid-driven cavity with Reynolds number 100 and 400. Let us discuss the domain of the test case. It is the unit cube cavity $(0,1) \times (0,1) \times (0,1)$ with the upper horizontal surface called the lid which is put into motion using the boundary con-

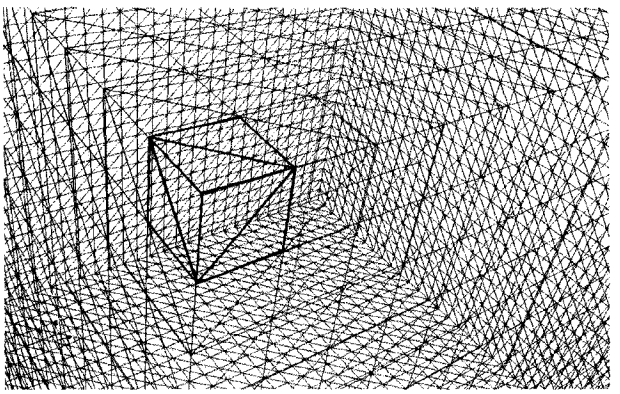

Figure 3.15: A close up of the mesh in 3 dimensions

dition $u(x, y, 1, t) = (0, U(t), 0)$ where $U(t)$ is a prescribed function. For the steady lid-driven case $U(t) = 1$. All other sides of the cavity (walls) are set to have a no-slip boundary condition meaning that $u = 0$ on the walls. The characteristic length and velocity are $L = 1$ and $V = 1$, respectively, which yields a Reynolds number of simply $\mathrm{Re} = 1/\nu$. The unit cube is divided into $N \times N \times N$ smaller cubes and then each smaller cube is divided into 6 tetrahedra. This mesh has $N \times N \times N \times 6$ elements. In figure 3.15 we can see a close up of the 3-dimensional mesh. We shall present results for two meshsizes, $30 \times 30 \times 30 \times 6$ and $50 \times 50 \times 50 \times 6$ using some of the best preconditioning techniques from section 3.1 for the iterative solver GMRES and when possible, the LU factorization method.

Results from Shankar and M. Deshpande [13] are presented in figure 3.16 and 3.17 for $\mathrm{Re} = 100$ and $\mathrm{Re} = 400$, respectively. Figures (a) of Shankar's results shows three cross section of the cube that are parallel to the direction of the flow. The streamlines on the cross sections of the (a) pictures show some resemblance to the 2D cases. Figures (b) show the cross sections that are perpendicular to the flow. Notice the position of the saddle point in (b) is about three quarters of the way up the z-axis for $\mathrm{Re} = 100$, whereas when $\mathrm{Re} = 400$ this saddle point appears to be in the middle

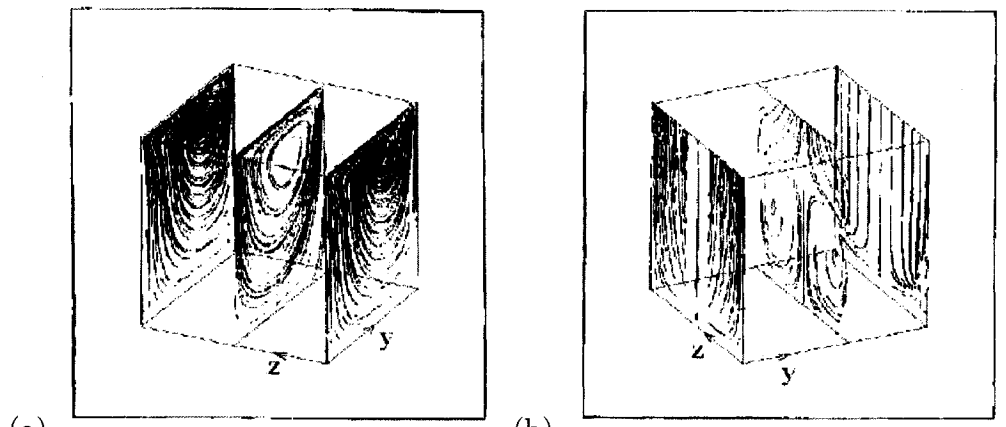

(a) (b)

Figure 3.16: The projections of the streamlines onto the end walls, side walls, and mid planes of the lid-driven cubic cavity with Re = 100 (from Shankar and M. Deshpande [13]). The lid moves in the y-direction .

of the mid plane. Another aspect one may look at is the positioning of the vortices on the back walls. These are the characteristics that we shall observe when running test cases with LU and preconditioned GMRES.

When running test cases on the 3D lid-driven cube (the lid is moving in the positive y-direction) we started with a meshsize of $30 \times 30 \times 30 \times 6$ and a Reynolds number of 100. Once again, toggling the number of KSPits and SNESits we were able to deduce some conclusions to compare the LU method with the preconditioned GMRES. Table 3.10 show the statistics for the computations done with different solvers for this test case. LU factorization takes up about 3369 Mb of memory and requires nearly 9 hours of CPU time for this test. When using the iterative solver GMRES and the appropriate preconditioner we can drastically reduce the amount of memory required and even the CPU time. For example, when using ILU(2) as a preconditioner we can obtain a result in less then one hour using only about 15% of the memory that was needed for LU factorization.

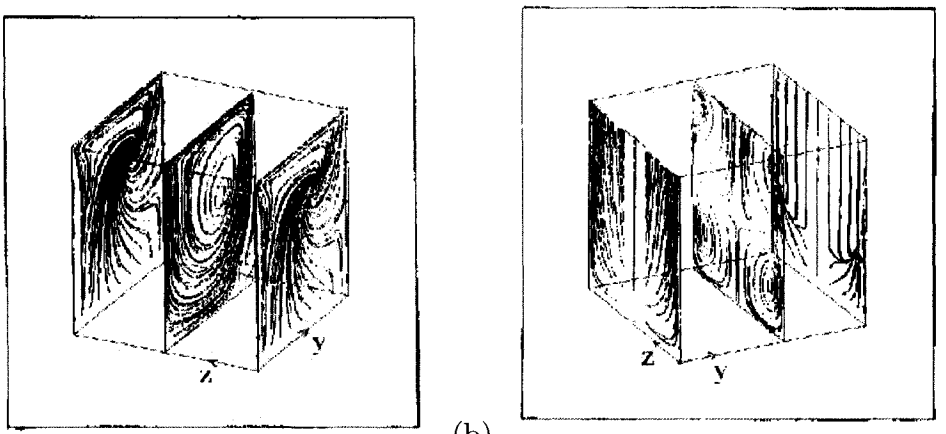

Figure 3.17: The projections of the streamlines onto the end walls, side walls, and mid planes of the lid-driven cubic cavity with Re = 400 (from Shankar and M. Deshpande [13]). The lid moves in the y-direction.

PC type	KSPits	SNESits	KSPres	SNESres	Mem(Mb)	CPU(min)
LU†	30	18 total	8.38×10^{-20}	2.69×10^{-15}	3369	534
Jacobi	30	5	1.40×10^{-05}	1.04×10^{-07}	162	256
ILU(0)	30	3	6.70×10^{-06}	1.92×10^{-09}	244	190
ILU(0)	100	5	4.57×10^{-06}	1.67×10^{-09}	244	312
ILU(1)	100	5	4.71×10^{-09}	1.41×10^{-09}	325	316
ILU(2)	30	2	1.23×10^{-12}	1.40×10^{-09}	479	122
ILU(2)†	30	1	7.39×10^{-09}	1.35×10^{-09}	479	54

Table 3.10: Numerical results for cavity size $30 \times 30 \times 30 \times 6$ with 10 timesteps of size 10 and Re = 100. Each uses GMRES except LU factorization.

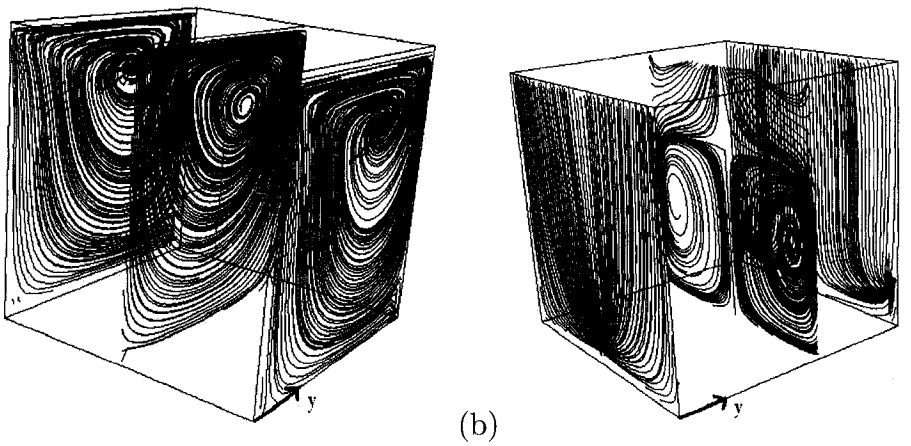

(a) (b)

Figure 3.18: The projections of the streamlines onto the end walls, side walls, and mid planes of the lid-driven cubic cavity of mesh size $30 \times 30 \times 30 \times 6$ with Re = 100 using LU factorization in PETSC. The lid moves in the y-direction.

The test cases marked with a † in table 3.10 are shown in figure 3.18 and 3.19. Figure 3.18 shows the simulation obtained when using LU factorization and figure 3.19 shows that the iterative solver GMRES with the ILU(2) preconditioner yields an identical result to that of the LU factorization. Both figures show similarity to the Shankar's results. The saddle point of the mid plane in (b) is nicely positioned and the vortices match well.

Now we shall change the Reynolds number from 100 to 400 and use the $30 \times 30 \times 30 \times 6$ mesh size once again. Table 3.11 shows the numerical data from a selected few test cases. We have narrowed down the amount of trials here using the best results from the previous test case. All three ILU preconditioners perform well here but ILU(2) is able to reach the smallest residual norm in the least amount of time. Figure 3.20 and 3.21 are the pictures obtained by the trials marked with a † from table 3.11. Note that on the end walls of the figures in (b) the streamlines exhibit some erratic behavior. This is due to the coarseness of the mesh and it dissipates when the mesh is refined to $50 \times 50 \times 50 \times 6$ which we will see next. Besides that flaw, the position

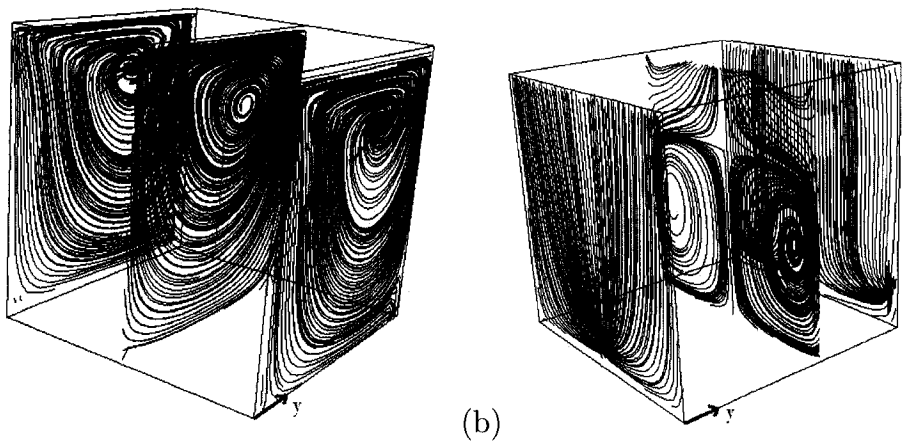

Figure 3.19: The projections of the streamlines onto the end walls, side walls, and mid planes of the lid-driven cubic cavity of mesh size $30 \times 30 \times 30 \times 6$ with Re = 100 using GMRES with ILU(2) preconditioner. The lid moves in the y-direction.

PC type	KSPits	SNESits	KSPres	SNESres	Mem(Mb)	CPU(min)
LU†	30	21 total	8.38×10^{-20}	2.69×10^{-15}	3369	534
ILU(0)	100	5	6.70×10^{-06}	1.92×10^{-09}	244	303
ILU(1)	100	5	4.71×10^{-06}	1.41×10^{-09}	325	316
ILU(2)†	30	1	6.97×10^{-06}	4.52×10^{-08}	479	54

Table 3.11: Numerical results for cavity size $30 \times 30 \times 30 \times 6$ with 10 timesteps of size 10 and Re = 400. Each uses GMRES except LU factorization.

of the saddle point of the mid plane is centered and vortices appear as they should based on Shankar's results.

The finest mesh tested in the 3D lid-driven cavity case was $50 \times 50 \times 50 \times 6$. The LU factorization was unable to function due to lack of memory and so the iterative solvers were put to work. In table 3.12 are several of the numerical results on this test case. We see that with this finer mesh, ILU(1) and ILU(0) are doing about as good as ILU(2) and so in figure 3.22 we have the result obtained using ILU(1) since this was the one with the lowest CPU time. We do not have a result for the LU factorization since there was not enough memory to do this calculation, but comparing the result

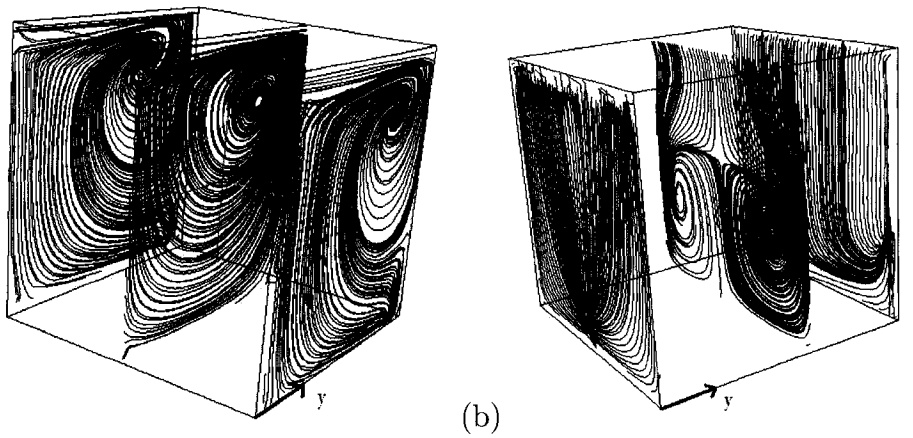

(a) (b)

Figure 3.20: The projections of the streamlines onto the end walls, side walls, and mid planes of the lid-driven cubic cavity of mesh size $30 \times 30 \times 30 \times 6$ with Re $= 400$ using LU factorization in PETSC. The lid moves in the y-direction.

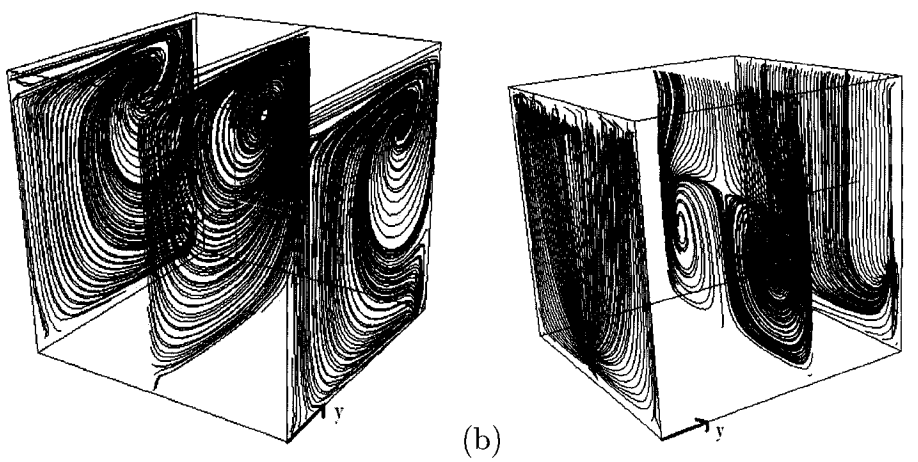

(a) (b)

Figure 3.21: The projections of the streamlines onto the end walls, side walls, and mid planes of the lid-driven cubic cavity of mesh size $30 \times 30 \times 30 \times 6$ with Re $= 400$ using GMRES with ILU(2) preconditioner. The lid moves in the y-direction.

PC type	KSPits	SNESits	KSPres	SNESres	Mem(Mb)	CPU(min)
LU	–	–	–	–	–	–
ILU(0)	30	1	6.70×10^{-06}	1.92×10^{-08}	1088	630
ILU(1)†	30	1	3.21×10^{-05}	2.46×10^{-09}	1461	621
ILU(2)	30	1	6.97×10^{-05}	4.52×10^{-09}	2188	666

Table 3.12: Numerical results for cavity size $50 \times 50 \times 50 \times 6$ with 10 timesteps of size 10 and Re = 100. Each uses GMRES except LU factorization.

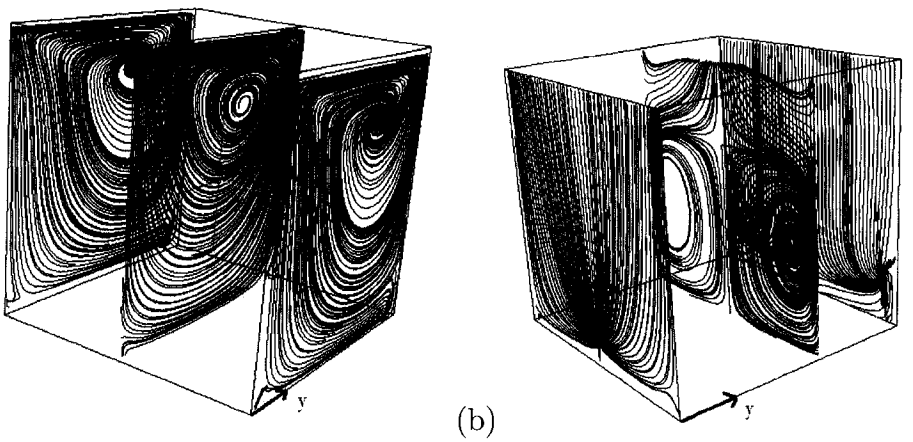

(a) (b)

Figure 3.22: The projections of the streamlines onto the end walls, side walls, and mid planes of the lid-driven cubic cavity of mesh size $50 \times 50 \times 50 \times 6$ with Re = 100 using GMRES and ILU(1) preconditioner. The lid moves in the y-direction.

of GMRES preconditioned with ILU(1), we see that it is nearly identical to Shankar's results.

Now we shall use the same meshsize but increase the Reynolds number to 400. Table 3.13 shows the statistics from this test case. The preconditioners ILU(0) and ILU(1) do satisfactory jobs but here we chose to show in figure 3.23 the result obtained using ILU(2) since it had the smallest residuals. Once again comparing this to Shankar's results we have nearly identical pictures.

Further investigation of the memory requirements for the 3D test cases shows that the jump from $N = 30$ to $N = 50$ requires about 4.5 times more memory when

PC type	KSPits	SNESits	KSPres	SNESres	Mem(Mb)	CPU(min)
LU	–	–	–	–	–	–
ILU(0)	30	1	9.33×10^{-04}	6.17×10^{-08}	1088	630
ILU(1)	30	1	2.96×10^{-05}	9.37×10^{-08}	1461	621
ILU(2)†	30	1	5.12×10^{-05}	5.06×10^{-09}	2188	683

Table 3.13: Numerical results for cavity size $50 \times 50 \times 50 \times 6$ with 10 timesteps of size 10 and Re = 400. Each uses GMRES except LU factorization.

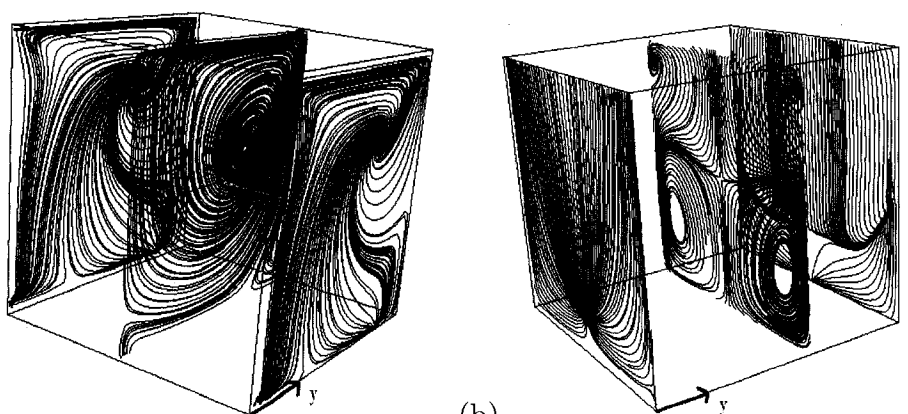

(a) (b)

Figure 3.23: The projections of the streamlines onto the end walls, side walls, and mid planes of the lid-driven cubic cavity of mesh size $50 \times 50 \times 50 \times 6$ with Re = 400 using GMRES and ILU(2) preconditioner. The lid moves in the y-direction.

N	# of Unknowns	LU	ILU(2)	ILU(1)	ILU(0)
30	227164	3369	479	325	244
50	1030604	> 8000	2188	1461	1088

Table 3.14: Memory requirements in Mb for cavity size $N \times N \times N \times 6$, Re = 100.

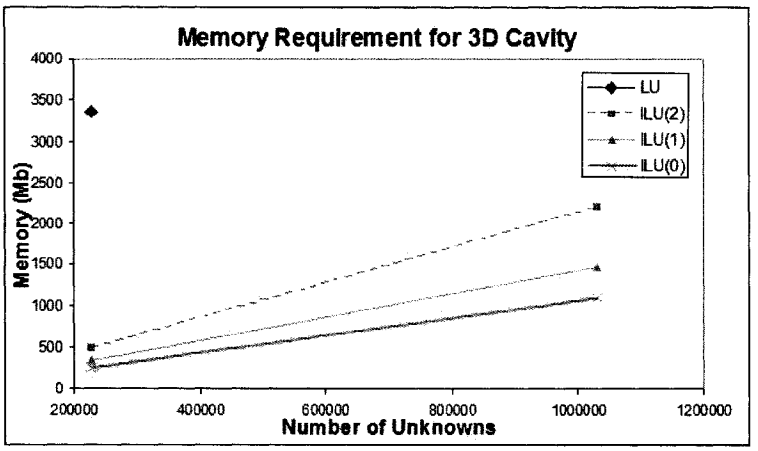

Figure 3.24: The memory requirements for the preconditioned GMRES using ILU(0), ILU(1), ILU(2) and LU factorization for cavity sizes $30 \times 30 \times 30 \times 6$ and $50 \times 50 \times 50 \times 6$ and Re = 100.

using the preconditioned GMRES. Table 3.14 summarizes the required memory of LU factorization and GMRES preconditioned with ILU(0), ILU(1) and ILU(2). The graph 3.24 shows the memory required versus the number of unknowns which was calculated for an $N \times N \times N \times 6$ mesh size with the formula $4((N+1)^3 + N^3)$.

Table 3.15 shows the CPU time required per Newton iteration for the 3D solvers. It was calculated by dividing the final CPU time by the total number of Newton iteration from that trial. Graph 3.25 reflects the data from the table just mentioned with the number of unknowns along the horizontal axis.

Table 3.16 summarizes the total CPU time required by some of the best results from this section and graph 3.26 shows how the LU factorization begins to take more time then GMRES as the number of unknowns gets larger.

N	# of Unknowns	LU	ILU(2)	ILU(1)	ILU(0)
30	227164	29.7	5.4	6.3	6.2
50	1030604	–	66.6	62.1	63.0

Table 3.15: CPU time (min) per Newton iteration for cavity size $N \times N \times N \times 6$, Re = 100.

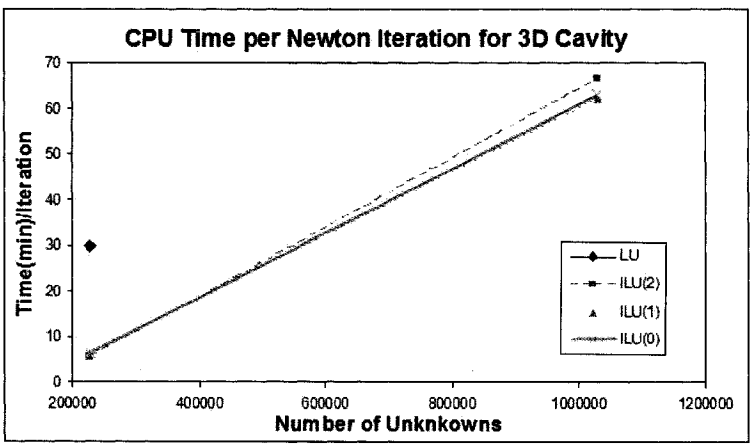

Figure 3.25: The CPU time per Newton iteration required for the preconditioned GMRES using ILU(0), ILU(1), ILU(2) and LU factorization for cavity sizes $30 \times 30 \times 30 \times 6$ and $50 \times 50 \times 50 \times 6$ and Re = 100.

N	# of Unknowns	LU	ILU(2)	ILU(1)	ILU(0)
30	227164	534	54	316	190
50	1030604	–	666	621	630

Table 3.16: Total CPU time for cavity size $N \times N \times N \times 6$, Re = 100.

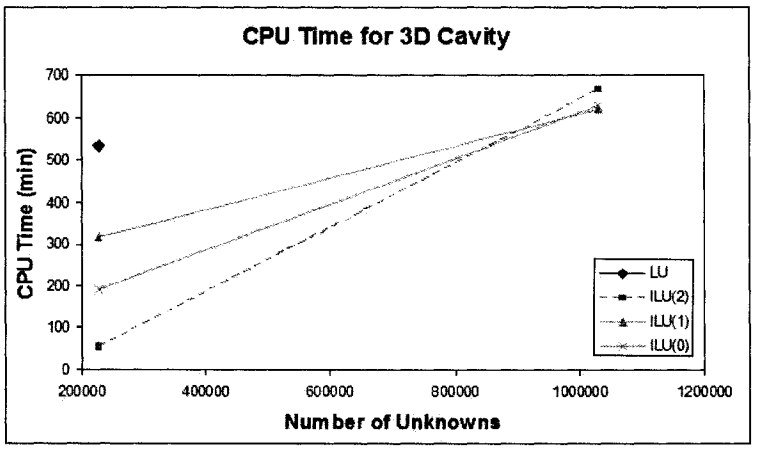

Figure 3.26: The total CPU time from the best results from the preconditioned GMRES using ILU(0), ILU(1), ILU(2) and LU factorization for cavity sizes $30 \times 30 \times 30 \times 6$ and $50 \times 50 \times 50 \times 6$ and Re = 100.

3.3 Results for a 2D Pulsating Lid-driven Cavity

We shall present some results obtained on a 2D square pulsating lid-driven cavity. This test case was analyzed in detail by C. Coros in [2], whose results confirm that using LU factorization on a meshsize $100 \times 100 \times 4$ and a stepsize of 0.01 yields accurate results. We shall once again use the unit square cavity $(0,1) \times (0,1)$ as the domain. The lid is put into motion using the boundary condition $u(x,1,t) = (U(t),0)$ where $U(t) = \cos(\frac{2\pi}{T}t)$ and T is the period of the moving lid. The walls are set to have a no-slip boundary condition. The characteristic length and velocity are $L = 1$ and $V = 1$, respectively, which yields a Reynolds number of simply Re= $1/\nu$ and a Strouhal number of Str= $1/T$. The mesh size used for all test cases will be $100 \times 100 \times 4$ and the stepsize will be 0.01.

The test case we chose to analyze is when Re = 1000 and Str= 1. This corresponds to a period of $T = 1$ time unit. The solvers run over an elapsed time of one period (1 time unit) which was chosen to be from $t = 10.0$ to $t = 11.0$. The results of

PC type	KSPits	SNESits	KSPres	SNESres	Mem(Mb)	CPU(min)
LU†	30	205 total	4.72×10^{-19}	3.32×10^{-12}	199	54
ILU(0)	30	10	7.23×10^{-07}	2.01×10^{-02}	65	121
ILU(1)†	100	5	2.09×10^{-07}	2.01×10^{-02}	81	107
ILU(2)	30	1	2.46×10^{-17}	2.01×10^{-02}	110	104

Table 3.17: Numerical results for cavity size $100 \times 100 \times 4$ with 100 timesteps of size 0.01 and Re = 1000, Str = 1 and $t = 11.0$. Each uses GMRES except LU factorization.

this test case are in table 3.17. When using the iterative solvers on the unsteady case we see that the linear solver is performing well, especially when the ILU(2) preconditioner is used with GMRES. The residual norm of the linear system is of the order $O(10^{-17})$. This precision is not necessary to obtain a reasonable result as we can see in figure 3.27,colored by the y velocity. LU factorization was used in (a) and the preconditioner ILU(1) along with GMRES was used in (b). Since we know LU factorization with stepsize 0.01 is reliable we shall use its result for comparison. The iterative solver GMRES with ILU(1) produces an identical result. The advantage to using the iterative solver here is that it conserves memory. To use the LU factorization for this test case requires 199 Mb of memory, whereas ILU(1) requires 81 Mb which is about 41% of what was needed for LU. The CPU time to use the iterative solver is about double what was needed to run the test case with LU factorization.

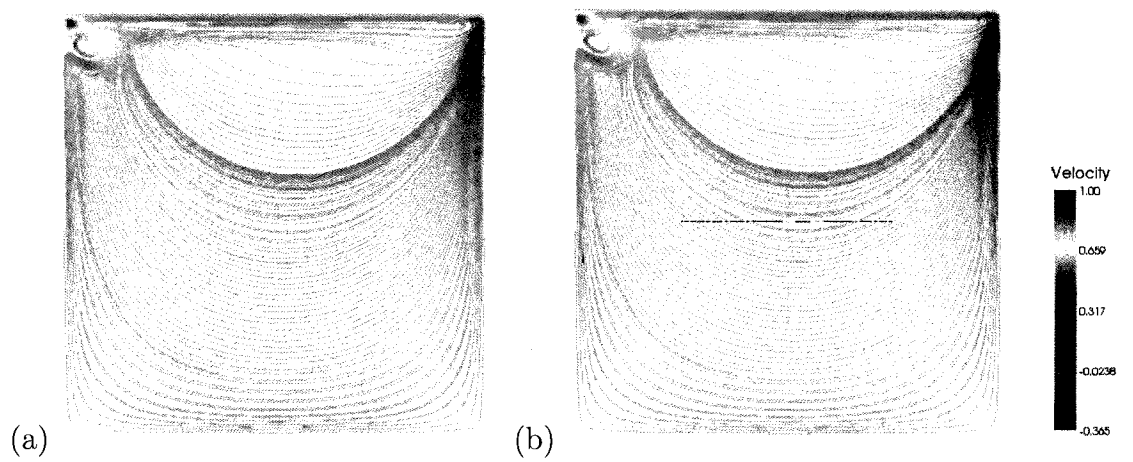

Figure 3.27: Pulsating unsteady lid-driven cavity with Re = 1000, Str = 1, t = 11.0 and Dt = 0.01 using (a) LU factorization and (b) the iterative solver GMRES with ILU(1) preconditioner

Chapter 4

Adaptive Time Stepping

4.1 Outline of the Method

Adaptive time stepping methods are used to control the discretization error by controlling the size of the time steps. The use of smaller timestep sizes results in more accurate results but at the cost of larger CPU times. One solution to optimize this compromise would be to derive a method that uses a timestep size that is re-calculated after each timestep to make the proper adjustments. This could ideally be more effective in solving our Navier–Stokes problem. There is a method proposed in [6] for a TR-BDF2 (TR for trapezoidal rule) adaptive time stepping scheme where TR is used for the first step, a "leapfrog" method is used to predict the velocity and then adaptive-BDF2 is used with the predictor as its first guess. To keep consistency within the code that was used to implement the constant stepsize test cases from Chapter 3, I have modified Gresho's proposed scheme to use a BE startup, the leapfrog predictor and then adaptive-BDF2 for the remaining steps.

Adaptive-BDF2 Time-Stepping Method

Startup

1. Select appropriate Δt_0 (small to ensure accuracy)

2. Take first time step with BE with $n = 0$ to get (U_1, P_1) with

$$\begin{bmatrix} \frac{1}{\Delta t_n} M + N(U_{n+1}) + K & B^T \\ B & 0 \end{bmatrix} \begin{bmatrix} U_{n+1} \\ P_{n+1} \end{bmatrix} = \begin{bmatrix} \frac{1}{\Delta t_n} M U_n + F_{n+1} \\ 0 \end{bmatrix} \tag{4.1.1}$$

3. Invert BE to get

$$\dot{U}_1 = \frac{U_1 - U_0}{\Delta t_0}$$

General Step

Take $\Delta t_1 = \Delta t_0$ and set $\omega_n = \frac{\Delta t_n}{\Delta t_{n-1}}$, for $n = 1, 2, ...$

1. Predict the velocity with "generalized Leapfrog"

$$U_{n+1}^p = U_n + (1 + \omega_n)\Delta t_n \dot{U}_n - \omega_n^2 (U_n - U_{n-1}) \tag{4.1.2}$$

2. Use BDF2 with variable time step to solve for (U_{n+1}, P_{n+1}) using U_{n+1}^p as the first guess.

$$\begin{bmatrix} \frac{(1+2\omega_n)}{\Delta t_n (1+\omega_n)} M + N(U_{n+1}) + K & B^T \\ B & 0 \end{bmatrix} \begin{bmatrix} U_{n+1} \\ P_{n+1} \end{bmatrix} = \begin{bmatrix} M\left(\frac{(1+\omega_n)}{\Delta t_n} U_n - \frac{\omega_n^2}{\Delta t_n (1+\omega_n)} U_{n-1}\right) + F_{n+1} \\ 0 \end{bmatrix} \tag{4.1.3}$$

3. Invert BDF2 to get

$$\dot{U}_n = \frac{3U_{n+1} - 4U_n + U_{n-1}}{2\Delta t_n}$$

4. Compute the local truncation error (LTE):

$$d_n = \frac{(1 + \omega_n)^2 \| U_{n+1} - U_{n+1}^p \|}{1 + 3\omega_n + 4\omega_n^2 + 2\omega_n^3}$$

5. Compute the next time step:

$$t_{n+1} = t_n + \Delta t_n$$
$$\Delta t_{n+1} = \Delta t_n * \min\left(\left(\frac{\epsilon}{d_n}\right)^{1/3}, 1+\sqrt{2}\right) \tag{4.1.4}$$

6. $n \leftarrow n+1$

Note that when $\Delta t_n = \Delta t_{n-1}$ the method simplifies to the constant step BDF2 scheme. When computing the next time step from the previous in 4.1.4 note that if the time step needs to be increased we must give an upper bound to this increase. In [9] the upper bound $\left(1+\sqrt{2}\right)$ is suggested to be appropriate. This upper bound is needed since when the LTE gets small, the term $(\epsilon/d_n)^{1/3}$ can become large depending on what the tolerance ϵ is. In order to perform step 2, of the general loop one would need an iterative method since this is an implicit, nonlinear equation. Newton's method works well to linearize the system and is what has been implemented. Once linearized there are even more methods to take into consideration to solve the systems since we will be dealing with very large, sparse matrices. We will need things like preconditioners and iterative solvers. In order to test out the adaptive time stepping scheme, the 2D steady lid-driven test case with mesh $100 \times 100 \times 4$ and Re $= 100$ and the 3D steady lid-driven test case with mesh $30 \times 30 \times 30 \times 6$ with Re $= 100$ will be analyzed.

4.2 Results of Adaptive Time Stepping on the 2D Lid-driven Cavity

As a first test on the adaptive-BDF2 time stepping scheme , the direct LU method was run with a constant time stepsize of 5 on the steady lid test case with a mesh of $100 \times 100 \times 4$ and with a Reynolds number Re $= 100$. Table 4.1 shows the results of

PC type	ϵ	DtSize	#Dt	KSPits	SNESits	KSPres	SNESres	Mem(Mb)	CPU(min)
LU†	–	5	20	30	26 total	2.30×10^{-18}	5.50×10^{-11}	187	6.0
LU†	1.0	Adap	5	30	13 total	2.58×10^{-18}	1.85×10^{-15}	187	2.7
ILU(0)	–	5	20	100	5	4.18×10^{-02}	1.07×10^{-03}	65	5.8
ILU(0)	1.0	Adap	6	100	5	1.67×10^{-02}	3.75×10^{-03}	65	2.4
ILU(0)	0.1	Adap	19	100	5	8.65×10^{-03}	7.92×10^{-04}	65	8.2
ILU(0)	0.01	Adap	31	100	5	2.33×10^{-04}	1.36×10^{-05}	65	20

Table 4.1: Numerical results for cavity size $100 \times 100 \times 4$ with $\mathrm{Re} = 100$ using constant and adaptive timestepping

some of these trials. If no value for ϵ is specified, then a constant timestep is being used and when the adaptive timestepping scheme is being used it will read "Adap" under the column "DtSize". With the constant stepsize we see from table 4.1 that by doing 20 steps of size 5 (to reach a final time of 100) the LU factorization takes about 6 minutes to get to its final results. When the adaptive time stepping scheme was applied, the initial time step was chosen to be 5 time units, but we see that only 5 steps were needed to reach the final time of 100 time units using a tolerance of 1.0. The CPU time is literally cut in half to about 3 minutes and we can see in figure 4.1 the results in table 4.1 marked with a †. The constant timestep is in (a) and the result of the adaptive timestep is in (b). Figure 4.2 shows how the adaptive timestepping scheme changes the size of the timestep when solving the discretized Navier–Stokes problem. The size of the time timestep grows after each iteration since the LU method produces results with residuals small enough to match the specified tolerance. The last iteration in this graph decrease but this is due to the cutoff at $t = 100$ as we do not want to surpass this final time. The fact that the LU factorization is able to produce accurate results on the steady case in just one timestep (as seen in section 3.1) was already indication that this should work well so this is why we next want to look at the improvement one can make using a combination of the iterative solver GMRES and the adaptive time stepping scheme.

We shall now show the results obtained when using a combination of iterative solvers

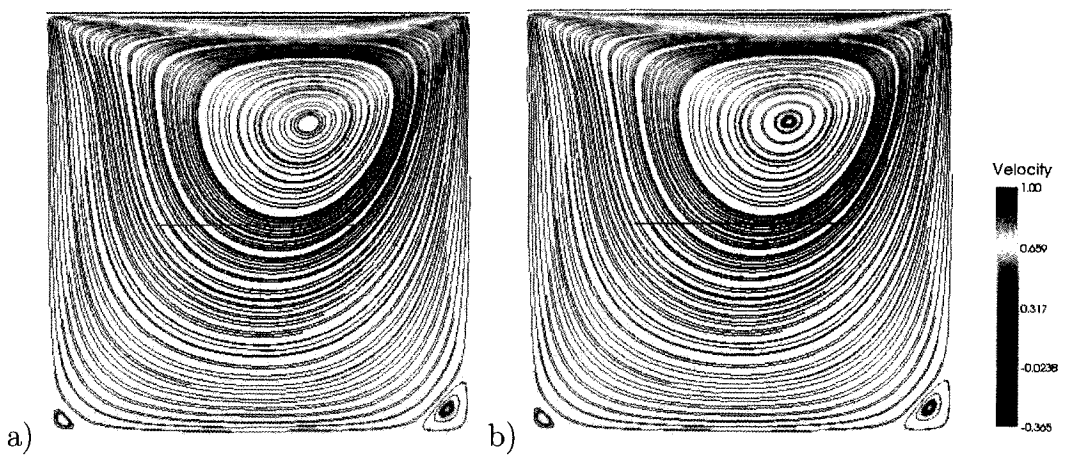

Figure 4.1: in figure (a) LU factorization with constant timestep is used, requiring about 6 minutes of CPU time whereas in figure (b) LU factorization with an adaptive timestep was used requiring only about 2.7 minutes of CPU time.

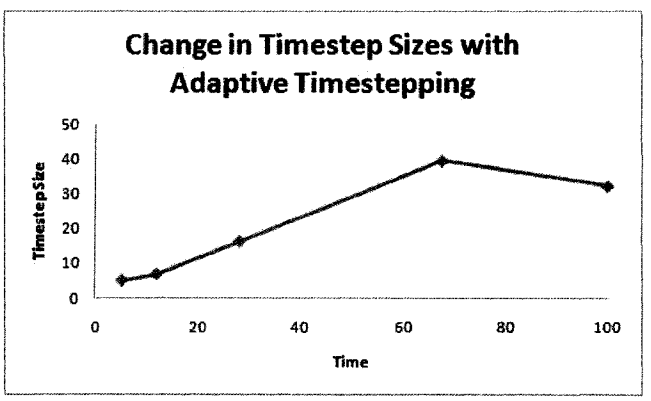

Figure 4.2: The size of the timestep size changes at each timestep with adaptive timestepping. Five timesteps were needed to arrive to the solution at $t = 100$ of the 2D steady lid-driven cavity

and adaptive times stepping. We shall use GMRES with 100 KSPits and 5 SNESits and we chose to use just one preconditioner, ILU(0), since results will follow a similar pattern for the other preconditioners. First we looked at what happens when we use 20 timesteps of constant size 5. As before when the stepsize was 10 (see section 3.1), the results are not good. Figure 4.3 shows all four results of the remaining test case from table 4.1 that are not marked with a †. Figure 4.3(a) is the result of GMRES, ILU(0) and constant timestep. Using the adaptive timestepping scheme with tolerance $\epsilon = 1.0$, shown in figure 4.3(b), we attain a result in about 2.4 minutes but the results are not any better then when the timestep was constant. Reducing the adaptive tolerance to 0.1 yields the result in figure 4.3(c) and we finally see some improvement in the quality of the solution, however the CPU time is growing and takes about 8.2 minutes. In figure 4.3(d) we see that with a tolerance of $\epsilon = 0.01$ we attain a solution identical to the good solution from the LU factorization but at the cost of an increased CPU time to about 20 minutes.

4.3 Results of Adaptive Time Stepping on the 3D Lid-driven Cavity

The adaptive time stepping scheme is next applied to the 3D steady lid-driven cavity with mesh $30 \times 30 \times 30 \times 6$ as described in chapter 3.1. Table 4.2 shows the statistics on these test cases. The direct LU method with constant timestep from section 3.3 is the first entry in table 4.2 and serves as a comparison point for the adaptive time stepping scheme. Figure 4.4 (a) is the result of the constant timestepping method with LU facotorization and shall be used for comparison with the others. We applied the adaptive timestepping scheme to the 3D cavity using the iterative solver GMRES with preconditioner ILU(0) and adaptive tolerance $\epsilon = 1.0$. Figure 4.4 (b) was obtained from this test and is the second entry in table 4.2 marked with a †. We see, however,

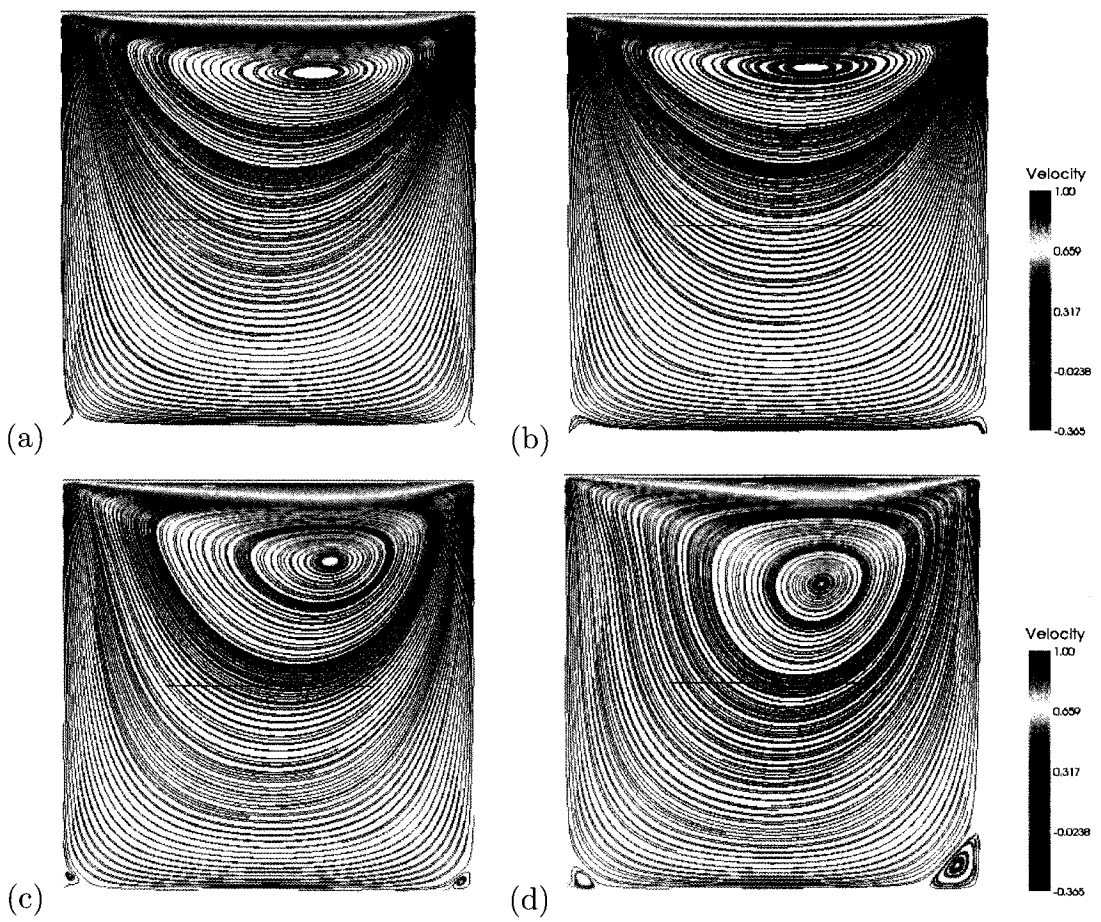

Figure 4.3: (a) GMRES with constant stepsize, (b) GMRES with adaptive timestepping with $\epsilon = 1.0$, (c) GMRES with adaptive timestepping with $\epsilon = 0.1$ and (d) GMRES with adaptive timestepping with $\epsilon = 0.01$.

PC type	ϵ	DtSize	#Dt	KSPits	SNESits	KSPres	SNESres	Mem(Mb)	CPU(min)
LU†	–	10	10	30	18 total	3.28×10^{-17}	2.69×10^{-17}	3369	560
LU	1.0	Adap	5	30	13 total	1.24×10^{-16}	2.13×10^{-14}	3369	588
ILU(0)	–	10	10	30	3	9.28×10^{-06}	7.79×10^{-09}	244	190
ILU(0)†	1.0	Adap	5	30	3	1.69×10^{-05}	1.43×10^{-08}	244	189
ILU(1)	–	10	10	100	5	4.71×10^{-09}	1.41×10^{-09}	325	316
ILU(1)	1.0	Adap	4	100	5	1.19×10^{-08}	3.22×10^{-06}	325	106
ILU(1)	0.1	Adap	5	100	5	1.11×10^{-09}	5.62×10^{-06}	325	110
ILU(1)	0.01	Adap	5	100	5	2.65×10^{-10}	1.08×10^{-06}	325	121
ILU(2)	–	10	10	30	1	7.39×10^{-09}	1.35×10^{-09}	479	54
ILU(2)	1.0	Adap	4	30	1	4.14×10^{-04}	4.37×10^{-06}	479	22
ILU(2)	0.1	Adap	4	30	1	2.82×10^{-04}	6.31×10^{-06}	479	22
ILU(2)†	0.01	Adap	5	30	1	1.05×10^{-04}	1.08×10^{-06}	479	24

Table 4.2: Numerical results for cavity size $30 \times 30 \times 30 \times 6$ with Re $= 100$ using constant and adaptive timestepping

that at this tolerance, the CPU time was not improved even though less timesteps were needed. Setting the tolerance to $\epsilon = 0.1$ for the ILU(0) preconditioner does not decrease the CPU time either since it forces the solvers to do an extra timestep. Next we applied the adaptive timestepping scheme to GMRES precondioned with ILU(1) and we once again see no significant improvement of the CPU times. Once we preconditioned GMRES with ILU(2) we begin to see some improvements and figure 4.4 (c) shows the result of this test with tolerance $\epsilon = 0.01$. GMRES with ILU(2) and a constant timestep takes about 54 minutes. Once the adaptive time stepping scheme is applied we get a CPU time of about 22 minutes, however we do sacrifice a few orders of precision on the residual norms.

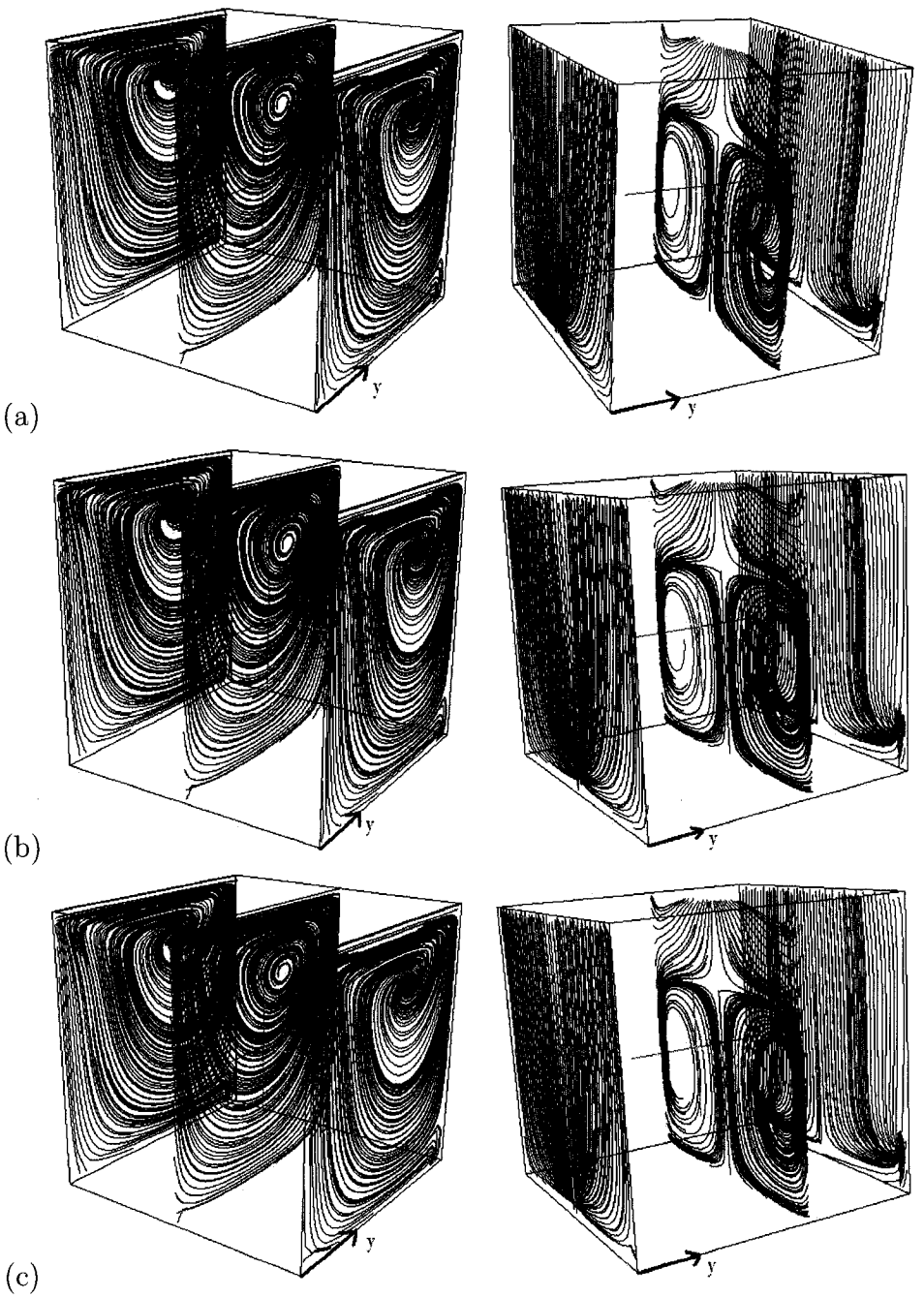

Figure 4.4: in figure (a) LU factorization is used requiring about 10 hours of CPU time to accomplish 10 timesteps of size 10. In figure (b) adaptive timestepping is used with GMRES and ILU(0) with tolerance $\epsilon = 1.0$. Figure (c) uses adaptive timestepping with GMRES and ILU(2) with tolerance $\epsilon = 0.01$

Chapter 5

Conclusions

Using iterative methods such as GMRES for solving the discretized Navier–Stokes equations clearly has its advantages as well as disadvantages. Several test cases were tried in this thesis in order to outline the characteristics of the direct solver LU factorization and the iterative solver GMRES.

We started out in 2D with a steady lid-driven square cavity and discovered that the iterative solver GMRES required many iterations in order to achieve a comparable accuracy to that of the direct LU factorization. The need for additional iterations for both the linear and nonlinear solvers resulted in an increased CPU time, but overall it is possible to achieve reasonable results using only a few more minutes than LU factorization if one is willing to sacrifice a few orders on the nonlinear residual norms. The benefit of the iterative solver clearly comes from the lower memory requirements, since running the preconditioned GMRES always required less megabytes than LU.

We tried the 3D steady lid-driven cavity and obtained very positive results. The CPU times and the memory requirement were cut dramatically and we now see the benefit of using the iterative solver GMRES on a flow problem. In 3D, direct methods

are less competitive because larger bandwidths in the sparsity pattern causes more nonzero elements to be created during the LU factorization. Iterative methods avoid such problems and are more efficient relative to the direct solver. We did sacrifice a few orders of precision on the residual norms by using the iterative solve but we see once the simulations were analyzed graphically that GMRES is just as good (if not better since it requires much less memory and CPU time) as the traditional direct method when solving the problem in 3D.

The iterative method GMRES was applied to the 2D unsteady lid-driven cavity and the best results using the preconditioners ILU(0), ILU(1) and ILU(2) were applied to this oscillating problem. As previously discovered about GMRES on the 2D problem, it can conserve memory but not always CPU time. Using ILU(0) as a preconditioner for this problem, one can obtain a very comparable solution to that of LU factorization due to the efficiency of the linear solver in this case.

In an attempt to eliminate the need to self-choose the size of the timestep required, an adaptive BDF2 timestepping scheme was implemented. It was tested on both the 2D ad 3D steady lid-driven cavities. Applying this adaptive time stepping scheme to the LU factorization method we were able to see the efficiency of the method. Given the size of the initial timestep, adaptive BDF2 will start increasing the stepsize right away (recall that LU factorization can solve the 2D steady-lid driven problem in just 1 timestep). It was more interesting to see what the effects were on the iterative solvers. In 2D we found that with ILU(0) preconditioner we could arrive to the same accuracy as was achieved with the constant timestepping in about half the time. We can then decrease the tolerance of the adaptive solver to achieve more precision but this resulted in more timesteps and hence higher CPU time. The CPU time of the most accurate results surpassed that of the LU factorization. We then applied the adaptive BDF2 to the 3D steady-lid driven problem. The results were positive as was

the case with the steady lid-driven cavity in 3D. We were successfully able to reduce the CPU time of the already fast iterative solver GMRES and maintain about the same accuracy.

Bibliography

[1] S. Balay, K. Buschelman, and more... **PetSc User's Manual**, Argonne National Laboratory, Argonne, 2007.

[2] C. Coros, Y. Bourgault , **On the numerical study of periodically forced 2-D cavity flows** International Journal for Numerical Methods in Fluids, Int. J. Numer. Meth. Fluids, Submitted.

[3] R. L. Devaney, **An Introduction to Chaotic Dynamical Systems**, The Benjamin/Cummings Publ. Co., 1986.

[4] A. Ern and J.-L. Guermond, **Theory and Practice of Finite Elements**, Applied Mathematical Sciences, Springer, 2005.

[5] U. Ghia, N. Ghia, C. Shin, **High-Re Solutions for Incompressible Flow Using the Navier-Stokes Equations and a Multigrid Method**, Journal of Computational Physics 48, 387-411, 1982.

[6] P. Gresho, D. Griffiths and D. Sylvester, **Adaptive Time-Stepping for Incompressible Flow Part I: Scalar Advection-Diffusion**, Society for Industrial and Applied Mathematics, *SIAM Journal of Scientific Computations* , Vol. 30, No. 4, pp. 2018-2054, 2008.

[7] P. Gresho and R. Sani, **Incompressible Flow and the Finite Element Method, Volume 2: Isothermal Laminar Flow**, John Wiley and sons, Ltd., 2000.

[8] E. Hairer, S.P. Norsett and G. Wanner, **Solving Ordinary Differential Equations I**, Second Revised Edition, Springer-Verlag, Berlin Heidelberg, 1993.

[9] E. Hairer and G. Wanner, **Solving Ordinary Differential Equations II**, Stiff and Differential-Algebraic Problems, Springer-Verlag, Berlin Heidelberg, 1991.

[10] Iwatsu R, Ishii K, Kawamura T, Kuwahara K,Hyun JM. **Simulation of transition to turbulence in a cubic cavity**. AIAA Pap. No. 98-0040, 1989.

[11] P. Kjellgren, **A semi-implicit fractional step finite element method for viscous incompressible flows**, Computational Mechanics 20: 541-550, 1997.

[12] Y. Saad, **Iterative methods for sparse linear systems** , Societey for Industrial and Applied Mathematics (SIAM), 2007.

[13] P. N. Shankar and M. D. Deshpande, **Fluid Mechanics in the Driven Cavity** Annu. Rev. Fluid Mech., 32:93136, 2000.